MODELLING THE AUXIN-MEDIATED VEIN FORMATION SYSTEM IN PLANT LEAVES

MARTIN JACOB (MARC) SLINGERLAND
B.Sc., University of Lethbridge, 2004
B.Ed., University of Lethbridge, 2004

A Thesis
Submitted to the School of Graduate Studies
of the University of Lethbridge
in Partial Fulfilment of the
Requirements for the Degree

MASTER OF SCIENCE

Department of Chemistry and Biochemistry
University of Lethbridge
LETHBRIDGE, ALBERTA, CANADA

Dedication

To Melinda,

who was willing
to let me play
for two more years.

Abstract

The plant hormone auxin is involved in a wide range of developmental phenomena in plants. It carries out many of its effects through a signalling network involving the regulation of specific genes, including those involved in its own polar transport between cells. These transporters are able to be redistributed between cell faces, causing the asymmetric auxin transport that is a key requirement for the formation of vein patterns in leaves. In this thesis I describe the development of a biochemical kinetics-based model of auxin signalling and transport in a single cell, which displays biologically plausible responses to auxin application. The single-cell model then serves as the basis for a multicell model of auxin-mediated vein formation at a very early stage of leaf formation in *Arabidopsis thaliana*.

Acknowledgements

I wish to thank my supervisor, Dr. Marc Roussel, for expressing his confidence by allowing me a remarkable degree of latitude in pursuing my project, for his constant support and guidance during both my undergraduate and graduate studies, and for his inspiring example as a scientist and teacher. Throughout my academic career, my family has provided sound foundations and constant support, for which I am very grateful.

Dr. Steven Mosimann first convinced me that a graduate degree might be a good thing to pursue, and played a large part in setting me on my current course. I value his friendship and good humour. He, Dr. Elizabeth Schultz and Quintin Steynen cheerfully fielded the endless questions that betrayed my woefully limited background in biology, and I thank them for stimulating and informative discussions on various aspects of my research. Dr. Andrew Hakin introduced me to the academic research environment, and Catharine Roussel provided invaluable assistance with programming and computer issues; I thank them both. David Franz and Kevin Davis survived sharing an office with me, and made my academic journey much more interesting. I also appreciate the friendship and mental stimulation offered by other students and researchers in the Roussel lab. It has been my privilege to interact with many other members of the U of L community, and I am thankful to them for enhancing the engaging and friendly environment that has been so important to my academic experience.

Finally, I gratefully acknowledge funding from the Natural Sciences and Engineering Research Council of Canada, the Alberta Ingenuity Fund, and the Keith and Hope Ferguson Memorial Scholarship.

Contents

List of Tables

List of Figures

Abbreviations and Conventions

The following abbreviations are used in this thesis:

2,4-D	2,4-dichlorophenoxyacetic acid
ABP1	auxin-binding protein1
AFB	auxin-signalling F-box protein
ARF	auxin response factor
AtHB8	*Arabidopsis thaliana* homeobox gene 8
AUX1	auxin-resistant1 (auxin influx transporter)
AuxRE	auxin-responsive DNA element
Aux/IAA	auxin/indole-3-acetic acid protein
AXR	auxin resistant (protein)
CP	convergence point
DE	differential equation
ECM	extracellular matrix
ER	endoplasmic reticulum
FD	facilitated diffusion
GFP	green fluorescent protein
GM	ground meristem
GUS	β-glucuronidase
IAA	indole-3-acetic acid (‘auxin’)
IBA	indole-3-butyric acid
LAX	like AUX1 (protein)
MDR	multiple drug resistance (protein)
NAA	1-naphthaleneacetic acid
NPA	1-*N*-naphthylphthalamic acid
PGP	P-glycoprotein
PID	pinoid (protein)
PIN	pin-formed (auxin efflux transporter)
PM	plasma membrane
PT	polar transport
RK4	fourth-order Runge-Kutta integrator
SAM	shoot apical meristem
TIR	transport inhibitor response (protein)

To refer to genes and proteins, the following conventions will be used: the gene *GENE-EXAMPLE1 (GEN1)* codes for protein product GEN1 (or Gen1), and *gen1* is a mutant form of the gene. Gene fusions of a promoter with a reporter are written as *promoter::reporter*; *e.g.*, *DR5::GUS* has the β-glucuronidase reporter gene under the control of the auxin-responsive DR5 promoter.

Chapter 1

Introduction

Plants have been appreciated from antiquity for their economic importance, their medicinal uses, and not least for their great beauty. Much of their aesthetic appeal is due to symmetry and other intricacies of form and pattern. The exquisite patterning of plants and other organisms is also important for their survival, and thus the study of biological patterns has historically been an area of great interest for the application of mathematical techniques such as modelling and simulation [1].

One striking feature of plant architecture is the network of veins visible in their leaves [2–6]. Veins are necessary both to import water and nutrients to leaf cells, and to remove wastes and photosynthetic products for distribution to other parts of the plant. While these vascular functions are common to all plant species, the precise arrangement of the veins can vary extremely widely (Fig. 1.1). Much of the study of plant development has been performed using mouse-ear or thale cress, a weed in the mustard family more commonly known by its systematic name, *Arabidopsis thaliana* [7–9]. Arabidopsis has long been used as a model organism for plant genetic, molecular and developmental research, due in large part to its short life cycle, prolific seed output, small size, and small, simple genome [8, 10, 11].

In arabidopsis, leaf vein pattern formation follows a characteristic course (Fig. 1.2), though with some variation depending on the stage of shoot development during which

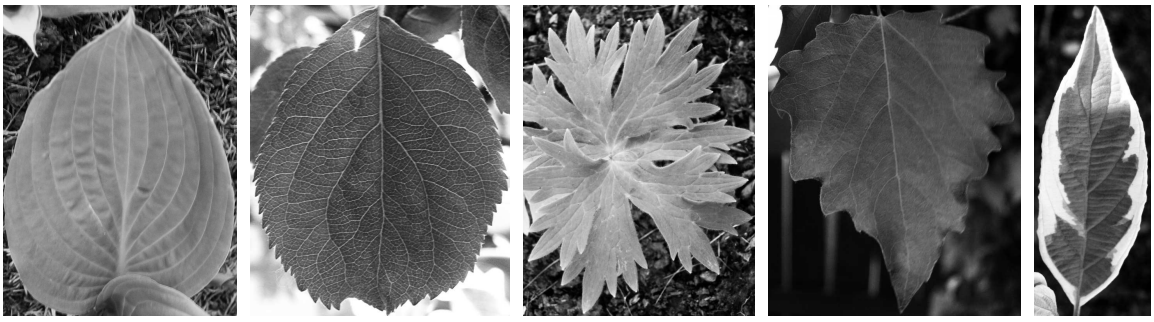

Figure 1.1: A variety of leaf venation patterns

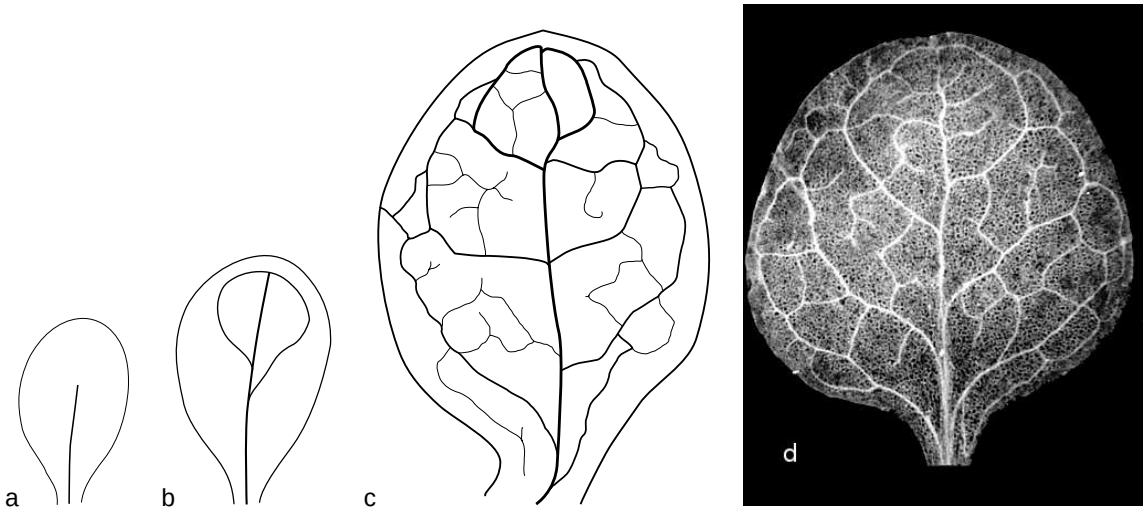

Figure 1.2: Sketch of arabidopsis vein formation progress (after [12]; not to scale). (a) (Primary) midvein only. (b) Midvein and first secondary vein loops. (c) Reticulated vein pattern in mature leaf. (d) Photo of arabidopsis leaf, courtesy Dr. E. Schultz.

the leaf forms [5, 12–16]. In the developing leaf primordium, a primary midvein forms acropetally (from the base to the tip of the leaf). The midvein then bifurcates and two secondary veins form near the edges of the leaf blade. Higher-order veins progressively differentiate, connecting both to themselves and to secondary vasculature. This process (secondary, then higher-order veins) is reiterated several times as the leaf blade matures basipetally. At maturity, veins of multiple orders are found throughout the entire lamina of the leaf.

The formation of these disparate vein networks is mediated by a plant (phyto-) hormone called indole-3-acetic acid (IAA) [14, 16–18], which has been found in all plants studied to date [19]. IAA is often referred to as auxin, since it is the most common member of a class of molecules with related structures known as auxins [20–22]. The structures of IAA and several other commonly studied auxins are depicted in Figure 1.3.

In arabidopsis and other plants, auxin has an impressive range of effects. Since the identification of the hormone by Went in the early twentieth century [23], it has been shown to be involved in cell expansion and division, vascular tissue specification and differentiation,

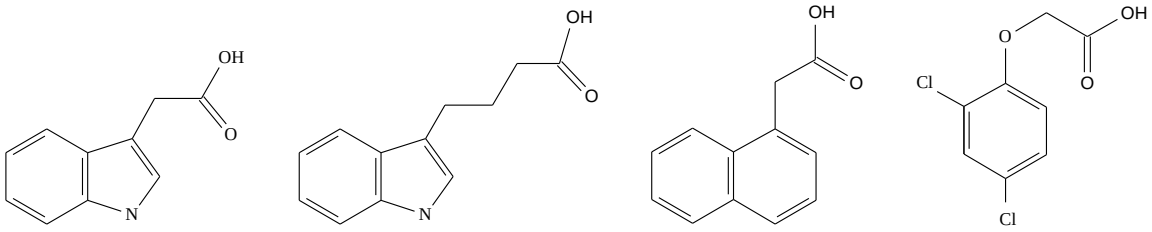

Figure 1.3: Structures of common auxins. From left to right: natural auxins, indole-3-acetic acid (IAA) and indole-3-butyric acid (IBA); synthetic auxins, 1-napthylacetic acid (1-NAA) and 2,4-dichlorophenoxyacetic acid (2,4-D).

root initiation, tropic responses, and various stages of fruit and flower development – in short, all plant tissues at all stages of development [19, 23–25].

Auxin is unique among known plant hormones in that it is actively moved between cells in specified directions by transporter proteins [26, 27]. Auxin is a weak acid, with a pK_a of about 4.8 [28]. In the intercellular space (pH $\approx$ 5.5), about 15% of auxin molecules are protonated and electrically neutral, and can therefore diffuse through the cell membrane into the cytoplasm. In the more basic cell interior (pH $\approx$ 7), the acidic proton is lost to yield anionic IAA^-, which is unable to diffuse out of the cell. This observation forms the basis of the long-standing 'chemiosmotic hypothesis' for auxin transport, which also postulates that the asymmetric distribution of auxin efflux transporters is largely responsible for the directionality of auxin transport (Fig. 1.4) [29, 30]. The chemiosmotic hypothesis [31] was first applied to explain auxin transport in the mid-1970s, and some alternative or complementary suggestions have since been put forward [32–38], but in large part recent work has merely supplied details about the molecular players involved in the remarkably prescient original hypothesis [39]. One important addition has been the realization of the importance of active auxin transporters, not diffusion alone, for auxin influx [28, 40].

The study of how auxin and its polar transport are involved in vein formation has revealed an intricately regulated system. Complex regulation is to be expected from a system that needs to be very plastic (the pattern must regenerate independently in each leaf, be able to adjust to environmental factors, and take on widely disparate forms in different

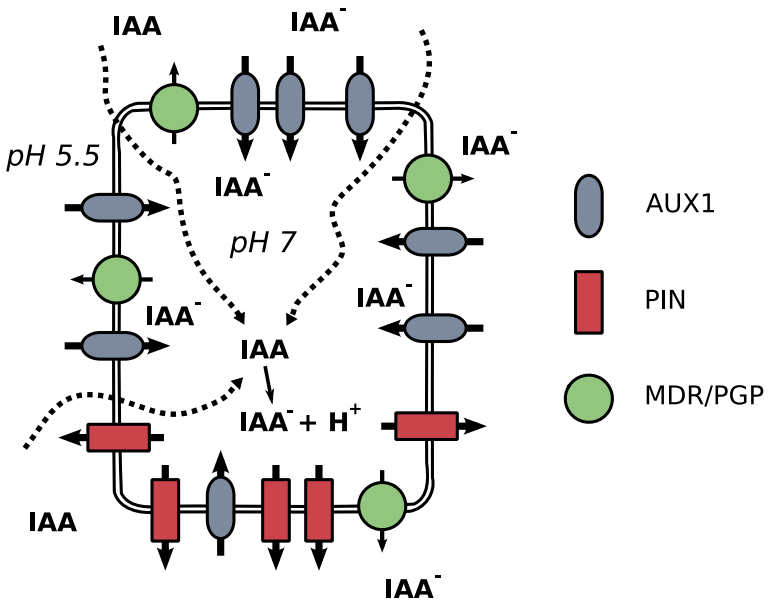

Figure 1.4: Schematic representation of the chemiosmotic hypothesis for auxin transport. Anionic auxin (IAA^-) is transported by specific carrier proteins (solid arrows). PIN and MDR/PGP are efflux carriers, while AUX1 is an influx transporter. Protonated auxin (IAA) is also able to diffuse from the extracellular space into the cell (dotted arrows), where it ionizes due to the higher internal pH.

species), but must always achieve a fully connected and functionally similar final state to be useful. Unfortunately, it is difficult to determine auxin location directly [38, 41], and so its presence must usually be inferred from its downstream effects. The sequence of vein formation referred to above (Fig. 1.2) relies on descriptions of one of those effects, the visible presence of morphologically distinct vascular elements [4]. These mature vascular cells are arranged in bundles composed of xylem (water-transporting) and phloem (organic material-transporting) elements; xylem has thickened cell walls, which make it easier to distinguish from neighbouring cells, and is often used to gauge vascular strand formation. The composition of vascular bundles is itself highly regulated, and exhibits polarity that is linked to the ad-/abaxial (upper/lower) polarity of leaves and to shoot apical meristem (SAM) patterning [3, 42–44]. The intricate arrangement of different cell types within leaf vasculature has been studied extensively [45–50], but will not be considered further here.

Fully differentiated cells are the last stage in vein formation, and we are interested not in the final state, but in how that stage is reached.

Future vascular cells, comprising the cambium (which will yield both xylem and phloem), are identifiable by their elongated, narrow shape; this morphology is first visible in the procambial (vascular meristematic) stage of development [51]. Even before this, though, cells have committed to eventual vascular fate, as evidenced by specific expression of marker genes. The stage when vascular cell specification has occurred but no anatomical changes are visible is referred to as either the pre-procambial or provascular stage of development [15, 51]. The progress of cellular development from unspecified ground meristem (GM) to prepro- to pro- to true cambium, and then through terminal differentiation, can be traced by the expression of various marker genes at specific developmental stages [15, 18, 52–54] and by morphological changes. Looking at the earliest possible stages of pattern formation is important, because very different ideas about auxin production, localization and flow direction can arise from observations of different stages. For instance, xylem in secondary vein loops appears to differentiate from the leaf tip downward [12]. Procambium formation, though, occurs nearly simultaneously along the entire loop, and the expression of pre-procambial marker AtHB8::GUS starts at an existing vein and extends upward [15]. Similarly, the midvein forms acropetally, despite a dependence on basipetal auxin flow [45, 55].

The involvement of auxin flow is a key feature in vein formation. An approach complementary to the vascular development markers mentioned above is the use of auxin-responsive promoters such as DR5 [56, 57] to visualize sites of high auxin activity, which to a large extent coincide with areas of vascular differentiation [18, 41]. The auxin transport system, especially the auxin efflux carrier PIN, also has a demonstrated involvement in vein formation and patterning [14, 17, 58–60]. Cells are marked by PIN and DR5 activation nearly a day before AtHB8::GUS expression becomes evident [16]. PIN expression is particularly interesting, because its polarity predicts auxin flow direction, and it is itself

regulated by auxin [61–63]. (See Section 2.2 for more on PIN.) A recent study of PIN localization in leaves concluded that the expression of PIN occurs at the time when pre-procambial cells are first being selected from the ground meristem [16]. In a mechanism similar to that proposed to operate in the meristem during phyllotaxis [64, 65], auxin produced in slightly older leaves [41] is transported through the epidermis and converges at a single site, where it is internalized and leads to PIN expression in subepidermal tissues. The subepidermal PIN is localized basally along the route of the future midvein. As the leaf grows, the same sequence of events is reiterated multiple times: auxin collects at an epidermal convergence point, which then becomes connected to the midvein by a zone of cells which gradually narrow to a single strand with basal PIN polarity, and finally the upper part of the loop develops in a similar manner [16]. Thus procambial development seems to occur along strands of tissue with a stable polarized auxin flow.

The observation of zones of auxin flow narrowing into single auxin-transporting files of cells is reminiscent of a classic series of experiments by Sachs, in which he showed that auxin flow is capable of inducing the formation of veins (in pea stems) [66]. On the basis of these experiments, Sachs proposed the 'canalization hypothesis' [67], which posits an autocatalytic feedback between auxin flow and auxin transport capacity. Cells with high levels of auxin flow undergo changes that make them more efficient at transporting auxin. When coupled with an asymmetry of efflux transporters, as in the chemiosmotic hypothesis, auxin produced in one zone becomes 'canalized' into files of cells specialized for auxin transport (Fig. 1.5) in a manner analogous to the formation of gullies by water drainage in soft terrain [68].

The canalization hypothesis provided the impetus for a series of modelling papers by Mitchison in the early 1980s [69–71]. Mitchison's models involve feedback between auxin flux and some parameter of the transport process. He first [69] considered purely diffusive auxin transport in an array of cells, with a linear auxin source and sink at the top and bottom of the array, respectively. Destabilization of an initially uniform linear flux gradi-

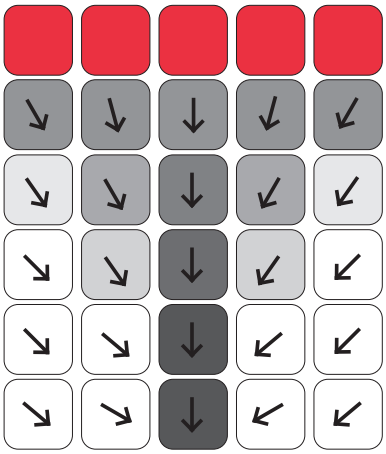

Figure 1.5: Schematic representation of the canalization hypothesis. Auxin produced in leaf margin cells (top row) is transported basally. Random variations in transport result in one cell having a slightly higher auxin flux than its neighbours. That cell thereby becomes better at transporting auxin, which induces higher flux in the cell directly below it, and so on. High-flux cells, since they rapidly export their auxin contents, become sinks for the auxin of neighbouring cells, and positive feedback results in a file of cells (a 'canal') with high auxin transport capacities. Cell shading indicates relative auxin flux intensity.

ent leads in this model to the formation of distinct channels of auxin flow from source to sink, provided the dependence of the diffusion coefficients on flux is more than linear. Incorporating growth into the cellular array allows the formation of branching flow patterns, and loops of vein could be generated by multiple interacting localized auxin sources or by moving sources. The pattern of these localized sources was suggested to perhaps be a product of activator-inhibitor patterning, changing in time with changes in leaf shape or size. Mitchison suggested that diffusion-based patterning, with a distributed and slow-changing auxin source, was an appropriate model for initial large-scale leaf patterning. Later, more rapidly changing local sources could effect vein patterning on a smaller scale. Mitchison's diffusion-based model was able to reiterate some phenomena observed by Sachs [66], such as the 'repellent' effect of nearby strands if both are carrying high auxin fluxes, and the formation of cross connections from new sources to previously formed strands with low flux.

Diffusion alone, however, cannot account for some observed phenomena, such as vein loops with circulatory flow. Mitchison therefore also considered models with polar auxin transport, particularly in a subsequent paper [71]. This model supposes auxin pumps or channels at one end of each cell, whose number or transport efficiency increases with increasing auxin flux. Again, transport efficiency must increase more than linearly with the flux if destabilization of an initially uniform flow pattern is to result in specific strands of cells with higher auxin transport capacity, which "may be regarded as precursors to veins". Under appropriate conditions (high auxin concentration), small loops of continuous auxin flow can also form, which was not possible for the purely diffusive model. In order for vein formation to occur in this model, cell polarity (given as the ratio of polar to diffusive transport) cannot be too large. The allowed polarity can be quite a bit higher, however, if the cell contains a large vacuole with an auxin-impermeable tonoplast. The effect of various configurations of such intracellular features on auxin transport velocities was also considered by Mitchison [70, 72, 73].

Recently, Rolland-Lagan and Prusinkiewicz investigated the ability of canalization-based models to account for various experimentally observed features of leaf vein formation, using Mitchison's facilitated diffusion (FD) and polar transport (PT) models as a basis [74]. New model variants introduced by these authors included an explicit separate term for passive diffusion, and the effects of various source and sink configurations were also investigated. The modelled variables are transport coefficients, interpretable as related to the number of available auxin transporters (or channels). Background and auxin flux-responsive production as well as degradation are included, with a set maximum coefficient for each. In both FD and PT models, transport capacity increases as a function of the square of auxin flux. As Mitchison found, the response of transport coefficients to changes in flux must be non-linear for canalization to occur. Simulation results do not directly show vein differentiation, but auxin fluxes. It is assumed that high auxin flux leads to differentiation, and so veins are defined as files of cells which have reached their maximum transport ca-

pacity, or which have average influx rate at least three times greater than a low-flux cell file. Auxin-transporting cell strands originally have a low auxin concentration (and high flux), but the concentration in the file can grow after the strand has formed.

Using simulations of the refined model, Mitchison's results were confirmed on larger cell arrays, and the model was extended to account for other features of leaf vein formation. With a line source and a single sink cell, it is possible for the model to reiterate the seemingly paradoxical acropetal (sink-driven) formation of the midvein, even with basipetal auxin transport [15, 45, 55]. Loops of secondary vein formation can also be simulated, either (in the FD model) by sink movement (simulating leaf growth) and the introduction of new auxin sources, or (in the PT model) with an extended auxin source and appropriate parameter values. Model results showing similarities to the effects of auxin transport inhibition or of vein continuity mutants can also be observed in appropriately configured simulations. It is suggested that localized auxin sources may be important in the formation of loops and of discontinuous vein segments. The role of background diffusion is also highlighted in these models, where it can be isolated from the effects of facilitated transport. With no background diffusion, even a single auxin source can lead to fairly closely spaced strands of high auxin flux. Diffusion increases the 'reach' of the strands; existing strands are able to serve as sinks to cells further away, reducing or preventing the formation of multiple strands.

Rolland-Lagan and Prusinkiewicz's canalization model [74] demonstrates at least the potential to form discontinuous vein segments. It has often been argued, however, that the existence of vein patterning mutants with discontinuous vasculature [75–78] implies the inadequacy of canalization alone to explain vascular pattern development [13, 77, 79]. Another type of model sometimes proposed to simulate formation of vein networks involves reaction-diffusion systems [80–83]. In a reaction-diffusion patterning system, a local peak of an activator (differentiation-promoting substance) is formed by autocatalysis. In response to the presence of the activator, an inhibitory substance is produced (or alter-

natively, another activator is depleted). Because the inhibitor diffuses more quickly than the activator, it keeps the activator from spreading. When activator production ceases as a result of differentiation, though, inhibitor production is also retarded. This releases the inhibitory effect on neighbouring cells; small (random) initial asymmetries can be amplified into preferred directions for the formation of a new autocatalytic activator peak that begins the process anew. The combination of local autocatalysis and long-range inhibition can generate a variety of patterns depending on the production and diffusion rates of the substances involved and the details of their interactions. Attractive features of the reaction-diffusion prepattern hypothesis for venation models are that the system displays a biologically realistic characteristic spacing, with new veins intercalated if necessary during growth. The simultaneous formation of higher-order veins has also been suggested to rely on a preexisting pattern possibly due to a reaction-diffusion mechanism [13].

Canalization models such as those by Mitchison and reaction-diffusion mechanisms discussed by Meinhardtwere for quite some time the two major choices for models of vein formation. The availability of increasing amounts of molecular data, though, especially in the last several years, and in particular the realization of the key role in pattern formation played by specific auxin transport [14, 16–18, 41], has led to the recent publication of numerous models studying various portions of the auxin system at a more-or-less molecular level. Of particular interest, several of these models investigate the interplay between auxin localization and its transport, the essence of the canalization hypothesis.

In one example of this, Feugier *et al.* performed a series of simulations on an ovoid lattice of around 3000 hexagonal cells [84]. Variables considered are auxin fluxes and efflux carrier concentrations for each cell face, and the internal concentrations of transporters, of auxin and of a hypothetical auxin-producing enzyme. Auxin is produced in all cells, and a single cell corresponding to the leaf petiole serves as a sink. Auxin efflux transporters are produced or reallocated based on the auxin flux through each cell face. Several model variants were constructed: auxin flux between cells is allowed to be either a linear

or saturating function of auxin concentration, and carrier proteins are considered either as being independently regulated at each cell face, or as having a fixed total number, competitively distributed to the cell faces from a central compartment. For each of the four combinations of these characteristics, nine different functional forms were considered for the dependence of PIN activity on (outward-directed) flux. Computer simulations of the resulting auxin transport models showed that branching patterns of veins (files of similarly oriented cells with high flux) could be formed when PIN response was accelerated (greater than linear) with respect to auxin flux. Interestingly, though, while the branched veins always had high auxin flux passing through them, they could form with either high or low auxin concentrations relative to the non-vein cells. The former case occurred when cell sides had to compete for a set pool of transporters; the latter when transporter levels were independently regulated at each cell face.

Under all conditions investigated in [84], only linear veins form, not connected loops. The same is true for a canalization model by Fujita and Mochizuki [85], which includes a dependence of PIN metabolism on the presence of a diffusible enhancer. This hypothetical enhancer is produced in each cell at a rate dependent on the auxin flux through that cell. The model shows branching vein formation under certain conditions, with a regular spatial organization due to the reaction-diffusion-like enhancer behaviour. With parameter values intermediate between branching and non-pattern-forming regimes, inhomogeneities can form without extending to global structure. Small closed paths of auxin flow are observed, but these are not 'vein loops' in the conventional sense, as they do not connect different parts of the leaf and are not formed by connecting pre-existing linear veins.

The formation of only branching vein patterns in several different canalization models, and the existence of venation mutants with open-ended veins [86, 87], led Feugier and Iwasa to suggest that the connection of veins to one another could be due to a process separate from that involved in vein formation [79]. They proposed a model based on the earlier one by Feugier *et al.* [84] with fixed total PIN in each hexagonal cell, linear auxin

flux, and PIN reallocation to a cell face depending on the square of the outward auxin flux through that face. In addition, however, an entity called 'flux-bifurcator' is introduced, whose presence is an indicator of strong auxin outflux (and likely vein identity) in a cell. If two cells both with high flux-bifurcator levels are near one another they can interact, with each cell reallocating auxin transporters to the side facing the other. Simulations (again with uniformly produced auxin) result in the formation of branching or reticulated patterns, depending on parameters. Discontinuous veins or loops of continuous flow may also result under certain conditions. The authors draw attention to the fact that no cells occur with flux out of two opposing ends; thus, though somewhat realistic venation patterns can be generated, there is a difference with experimental data from Scarpella *et al.* [16], who found such a bipolar cell in every (secondary) vein loop.

In addition to the work already cited, there are many other models examining aspects of auxin-related phenomena in plants. So, for instance, models have been developed to reconcile theories of polar auxin transport through linear files of cells with experimental observations in stem sections [88–90], to simulate auxin transport-mediated patterning in trees [91, 92], to examine the interplay of vein patterning with leaf blade growth [6, 93], and to study the feasibility of diffusion-based patterning of the area within an existing vein loop [94]. Venation models using cellular automata [95] or biomechanical stresses [96, 97] have been proposed. Another well-known patterning phenomenon in plants, leaf phyllotaxy (the arrangement of leaves around the stem), has also been modelled by various groups – particularly within in the past year [81, 98–103]. While the levels of detail in these model treatments vary, most examine only a few cellular variables explicitly. The effects of other necessary components are incorporated either through simulation conditions, or by introducing hypothetical substances to generate the necessary effects. It is therefore often difficult to interpret these models in terms of the biochemical components involved in auxin-mediated patterning. Of course, including more molecular detail increases the complexity and the number of parameters in a model, making full exploration of state

space unrealistic. But this disadvantage is outweighed by the possibility of investigating a range of cellular phenomena at a molecular level, as well as more facile comparison with known mutants.

To my knowledge, no mathematical model for vein patterning has yet been developed that includes both the transport of auxin and the signalling mechanism that responds to it, despite the close connection between the two systems [62, 104, 105]. A great deal of genetic and biochemical data relevant to both auxin transport and auxin signalling has been published in recent years. My goal in this thesis has been to incorporate known intermolecular interactions into a fairly comprehensive model incorporating both the auxin signalling and transport networks involved in the very earliest stages of vein pattern formation. Performing and analyzing simulations with this model affords insights into the vein patterning network in plants, and provides a convenient way to abstract this complex system from the even greater complexity of auxin's effects in plants.

Chapter 2

Model Description

As described in the Introduction, auxin occupies a very important position in plant biology. Thanks to the concerted efforts of research groups around the world, an understanding of how auxin achieves its effects has begun to come into focus over the past several years. Recent overviews of auxin biology can be found in, *e.g.*, [105–112].

One of the disadvantages of auxin's pleiotropic effects is that it is often difficult to separate a single phenomenon or gene of interest from the many related processes that are also affected. This is a major motivation for developing a mathematical version of the auxin system: it enables examination of cellular changes at a higher resolution than is available in the laboratory [113–115]. An added benefit, of course, is that many different conditions can be simulated in a short time, without the limitations imposed by growth and handling of real plants.

Conceptually, the auxin system in plants can be thought of in two separate but interacting parts: the signal transduction pathway by which auxin influences cellular activity, and the mechanism of its transport between cells. This chapter provides a summary of the molecular interactions involved in auxin biology, and describes how these interactions have been incorporated in a mathematical model.

2.1 Auxin Signalling

Most biological signalling pathways begin with a cellular receptor recognizing a stimulus, which is then transduced into some effect(s) [107, 116]. A logical way to begin the study of auxin signalling, then, was to identify an auxin receptor. This had already been done in the 1970s with the initial characterization of auxin-binding protein 1 (ABP1) [117]. ABP1 is essential for plant growth, and seems to be linked to early auxin responses, including ion channel and voltage changes at the plasma membrane [118]. Most ABP1 is ER-localized,

though, and despite extensive study its roles and mechanisms remain far from clear [119–122].

Considerably more is known about responses not involving ABP1, especially auxin's effects on gene expression. Several characterized gene families display rapid expression increases (within minutes) upon the application of auxin [123]. Rapidly auxin-induced genes are identified by auxin-responsive elements (AuxREs) in their promoter regions [124, 125]. Transcription factors known as auxin response factors (ARFs) bind to these AuxREs [124, 126, 127]. The earliest known and best-characterized of the 22 arabidopsis ARFs act as transcriptional activators. It has since been found that only those ARFs with glutamine-rich middle regions are activators [128], but the function of repressing ARFs is less clear [129]. Interactions between ARFs are also possible, but to limit the complexity of our model we consider only a single ARF species, acting as an activator.

Single ARF binding is insufficient for transcriptional activation (or possibly for a basal level of transcription) [129, 130]. Dimerization of DNA-bound ARFs through their N-terminal domains III & IV is required to induce full transcription of auxin-responsive genes [105]. We assume every ARF binding site to be constantly occupied (*i.e.*, initial ARF binding to DNA is strongly favoured), and so only the pool of DNA with an ARF already bound must be explicitly considered. This simplification still allows for the inclusion of constitutive gene transcription.

$$\mathrm{ARF} + \mathrm{ARF/DNA} \underset{k_1^-}{\overset{k_1^+}{\rightleftharpoons}} \mathrm{ARF}_2\mathrm{/DNA} \tag{2.1}$$

Once ARFs are dimerized on the promoters of auxin-responsive genes, transcription commences. Both transcription and translation are rapid processes compared to other characteristic time scales of the system, and thus gene product accumulation is modelled as instantaneous upon ARF dimerization. Numerous cellular factors – promoter strength, mRNA copy number, post-transcriptional modifications, etc. – influence gene transcription

and translation, and in general these effects will differ for different genes. Therefore, the production rate for each of the auxin-regulated species in the model is specified separately.

$$\begin{aligned} \mathrm{ARF_2/DNA} &\xrightarrow{k_{2,AUX}} \mathrm{ARF_2/DNA + AUX1} \\ \mathrm{ARF_2/DNA} &\xrightarrow{k_{2,PIN}} \mathrm{ARF_2/DNA + PIN_{in}} \\ \mathrm{ARF_2/DNA} &\xrightarrow{k_{2,x}} \mathrm{ARF_2/DNA + Aux/IAA} \end{aligned} \tag{2.2}$$

AUX1 is an auxin influx transporter; PIN is an auxin efflux transporter. Both are discussed further in Section 2.2, dealing with auxin transport. The third auxin-responsive gene product considered in reactions (2.2) is a member of a family of early auxin-responsive gene products known as the auxin/indole-3-acetic acid (Aux/IAA) proteins [123, 131], which are key actors in auxin signalling. Like ARFs, Aux/IAAs include domains III and IV, and so can heterodimerize with ARFs. This heterodimerization may occur by way of competitive binding of Aux/IAAs to free ARFs, reducing the number of free ARFs available to homodimerize on AuxREs [132]; alternatively, Aux/IAAs may bind to ARFs already on DNA promoters, and physically impede ARF access. Either mechanism leads to a reduction in ARF homodimerization, thus preventing auxin-responsive transcription (reactions (2.1) and (2.2)).

$$\begin{aligned} \mathrm{Aux/IAA + ARF} &\underset{k_3^-}{\overset{k_3^+}{\rightleftharpoons}} \text{inactive dimer} \\ \mathrm{Aux/IAA + ARF/DNA} &\underset{k_4^-}{\overset{k_4^+}{\rightleftharpoons}} \text{inactive DNA} \end{aligned} \tag{2.3}$$

It is also possible for Aux/IAAs to homodimerize, reducing the number of free Aux/IAAs in solution [133].

$$\mathrm{Aux/IAA + Aux/IAA} \underset{k_5^-}{\overset{k_5^+}{\rightleftharpoons}} \mathrm{(Aux/IAA)_2} \tag{2.4}$$

Aux/IAA proteins are rapidly turned over within plant cells [134], and their function depends upon this dynamic instability. Upon the application of auxin, Aux/IAAs are degraded by the 26S proteasome [135]. This degradation relies upon the ubiquitination of the Aux/IAAs by an E3 ubiquitin ligase, SCF^{TIR1} [136–138]. Auxin binding to the TIR1 (or related AFB1-3) protein of the SCF^{TIR1} complex directly promotes Aux/IAA ubiquitin tagging within 5 minutes [106, 130, 139–142]. We model the ubiquitination of Aux/IAAs by a Michaelis-Menten-type equation; the maximal tagging speed depends on the efficiency of the SCF^{TIR1} E3 complex, which is activated by auxin. For simplicity, tagging and degradation are treated together; in essence, we treat the degradation of Aux/IAAs as instantaneous once the ubiquitin tagging has occurred.

$$\mathrm{Aux/IAA} \rightarrow \qquad v_6 = \frac{k_6 K_{SCF}[\mathrm{auxin_{in}}][\mathrm{Aux/IAA}]}{(1+K_{SCF}[\mathrm{auxin_{in}}])([\mathrm{Aux/IAA}]+K_{6m})} \tag{2.5}$$

As tagged Aux/IAAs are degraded in response to auxin, they release ARFs (reactions (2.3)), which are then free to homodimerize and elicit transcriptional responses (reactions (2.2)).

2.2 Auxin Transport

In order to bind to TIR1 and effect signalling, auxin must of course first enter the cell. We restrict our attention to specific polar transport, which relies on the action of dedicated transport proteins. AUXIN-RESISTANT1 (AUX1) seems to be the major influx transporter [143, 144], along with related (so far uncharacterized) LIKE AUX1 (LAX) gene products [145–147]. Members of the PIN-FORMED (PIN) protein family function as efflux transporters [63, 148–151], as do MULTI-DRUG RESISTANCE/P-GLYCOPROTEIN (MDR/PGP) proteins [150–153]. AUX1 and the PINs are by far the most well-studied transporters, and so our model includes AUX1 and a single PIN species (most likely PIN1 in leaves [16]). Note (reactions (2.2), above) that auxin-responsive control of both transporter-coding genes is allowed for in our model.

Both influx and efflux are treated in a similar way, with Michaelis-Menten kinetics. Auxin on one side of the plasma membrane reversibly binds to a transporter (AUX1 or PIN), forming an enzyme-substrate complex (labelled C1 or C2, respectively). The transporter then releases the auxin on the opposite side of the membrane. This mechanism is simplified (*e.g.*, it doesn't consider transporter structural changes or the possibility of transporter complexes rather than single enzymes) but it accurately models phenomena such as transporter saturation. Auxin transport processes are considered to be irreversible, as there is no experimental evidence for bidirectional auxin transport by either family of proteins. This may be related to auxin's different ionization states on either side of the cell membrane (see below.) Polarity of transport implies a difference between various cell faces, and we therefore treat the transporter concentrations in each face of the cell separately. Modelled cells are rectangular, with the cell sides and adjacent extracellular spaces labelled *a*-*d* for the top, left, right, and bottom of the cell, respectively (Fig. 2.1).

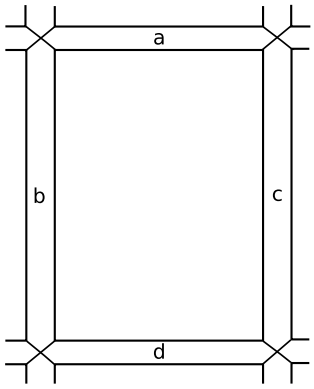

Figure 2.1: A single leaf cell, showing the extracellular spaces between it and neighbouring cells. Labels *a* – *d* identify regions of extracellular space and the adjacent cell faces.

$$\begin{aligned} \mathrm{AUX1_j} + \mathrm{auxin_{out,j}} &\underset{k_{7a}^-}{\overset{k_{7a}^+}{\rightleftharpoons}} \mathrm{C1_j} \overset{k_{7b}}{\longrightarrow} \mathrm{AUX1_j} + \mathrm{auxin_{in}} \qquad \mathrm{j} = a,b,c,d \\ \mathrm{PIN_j} + \mathrm{auxin_{in}} &\underset{k_{8a}^-}{\overset{k_{8a}^+}{\rightleftharpoons}} \mathrm{C2_j} \overset{k_{8b}}{\longrightarrow} \mathrm{PIN_j} + \mathrm{auxin_{out,j}} \qquad \mathrm{j} = a,b,c,d \end{aligned} \tag{2.6}$$

AUX1 and PIN transporter proteins may also be constantly degraded. Note that PINs are assumed not to be removed directly from the plasma membrane, but from an internal pool

of PIN proteins (PIN_{in}, discussed below), which is not directly involved in transport.

$$\begin{array}{r} \overset{k_9}{\text{AUX1}} \longrightarrow \\ \\ \overset{k_{10}}{\text{PIN}_{\text{in}}} \longrightarrow \end{array} \tag{2.7}$$

PINs have been shown to constantly cycle between the plasma membrane (PM) and internal compartments in an actin-dependent manner [62, 154–158], and it is this constitutive cycling that allows for development and realignment of auxin transport polarity. *In planta*, AUX1 also undergoes constitutive cycling and is asymmetrically localized in in some root tissues [147, 150, 159, 160] and in the shoot apical meristem [65, 101]. However, AUX1 polarity has not been demonstrated for leaf mesophyll, and in the current model PINs are considered to be the only polarized species, as originally suggested by the chemiosmotic hypothesis for auxin transport [29, 30, 39]. It would be interesting to investigate the effect of polarized auxin influx, particularly if the model were extended to non-leaf cells, but such study is beyond the scope of the current work.

Asymmetrical auxin transport polarity is achieved in our model by targeting PIN proteins preferentially to certain regions of the plasma membrane in a manner dependent on the auxin concentration external to each face. (Recall that for computational simplicity, we consider only a single type of PIN.) This requires separate rates for internalization and externalization of PINs. In the absence of detailed knowledge of cellular mechanisms for external concentration sensing, the rate of PIN exocytosis to each face of the plasma membrane, $v_{out,j}$, is given an arbitrary formulation which can be modified (by changing the exponent n) to instantiate different forms of auxin dependence of the exocytotic rate. The effects of changing n are considered in Section 3.7. PINs are re-internalized at a constant rate from the PM to an internal pool (PIN_{in}), which is also where PINs originally

accumulate when produced (reactions (2.2)).

$$\begin{array}{ll} \mathrm{PIN_{in}} \rightarrow \mathrm{PIN_j} & v_{out,j} = \dfrac{k_{out}[\mathrm{PIN_{in}}]}{1+\left(\frac{[\mathrm{auxin_{out}}]_j}{K_t}\right)^n} \\ \mathrm{PIN_j} \rightarrow \mathrm{PIN_{in}} & v_{in,j} = k_{in}[\mathrm{PIN}]_j \end{array} \qquad j = a,b,c,d \tag{2.8}$$

The protonated form of auxin, which exists to some extent at the relatively low pH of the intercellular space, can diffuse into cells. Diffusion is also possible between adjacent regions of the extracellular space. Cytoplasmic auxin is nearly completely deprotonated due to an elevated internal pH, and therefore can not diffuse out of the cell [144, 161].

$$\begin{array}{ll} \mathrm{auxin_{out,j}} \xrightarrow{k_{11}} \mathrm{auxin_{in}} & j = a,b,c,d \\ \mathrm{auxin_{out,j}} \xrightarrow{k_{ECM}} \mathrm{auxin_{out,k}} & j = a,b,c,d;\ \mathrm{k} = \text{neighbours of j} \end{array} \tag{2.9}$$

2.3 Model Equations

The model description outlined in the previous sections can be formulated mathematically as a set of differential equations (DEs). Most of the equations are derived from mass-action kinetics, with enzyme-mediated steps following Michaelis-Menten-type kinetics, as described. The rates of auxin addition and removal used in simulations are given by f_{in} and f_{out}, respectively. The full set of DEs corresponding to the described model system is given below. (As above, the four sides of the cell are labelled *a* through *d*; the 'neighbours' of a side are the sides adjacent to it (see Figure 2.1).)

$$\frac{d}{dt}[\mathrm{auxin_{in}}] = \sum_{j=a}^{d}\left\{\frac{k_{7b}[\mathrm{AUX1}]_j[\mathrm{auxin_{out}}]_j}{[\mathrm{auxin_{out}}]_j + K_{m1}} - \frac{k_{8b}[\mathrm{PIN}]_j[\mathrm{auxin_{in}}]}{[\mathrm{auxin_{in}}] + K_{m2}} + k_{11}[\mathrm{auxin_{out}}]_j\right\}$$

$$\frac{d}{dt}[\text{auxin}_{\text{out}}]_{\text{a}} = \text{f}_{\text{in}} - \frac{k_{7b}[\text{auxin}_{\text{out}}]_{\text{a}}[\text{AUX1}]_{\text{a}}}{[\text{auxin}_{\text{out}}]_{\text{a}} + K_{m1}} + \frac{k_{8b}[\text{auxin}_{\text{in}}][\text{PIN}]_{\text{a}}}{[\text{auxin}_{\text{in}}] + K_{m2}} - k_{11}[\text{auxin}_{\text{out}}]_{\text{a}} + \sum_k \{k_{ECM}[\text{auxin}_{\text{out}}]_{\text{k}}\} \qquad \text{k} = b, c$$

$$\frac{d}{dt}[\text{auxin}_{\text{out}}]_{\text{j}} = -\frac{k_{7b}[\text{auxin}_{\text{out}}]_{\text{j}}[\text{AUX1}]_{\text{j}}}{[\text{auxin}_{\text{out}}]_{\text{j}} + K_{m1}} + \frac{k_{8b}[\text{auxin}_{\text{in}}][\text{PIN}]_{\text{j}}}{[\text{auxin}_{\text{in}}] + K_{m2}} - k_{11}[\text{auxin}_{\text{out}}]_{\text{j}} + \sum_k \{k_{ECM}[\text{auxin}_{\text{out}}]_{\text{k}}\}$$
$$\text{j} = b, c; \ \text{k} = \text{neighbours of j}$$

$$\frac{d}{dt}[\text{auxin}_{\text{out}}]_{\text{d}} = -\frac{k_{7b}[\text{auxin}_{\text{out}}]_{\text{d}}[\text{AUX1}]_{\text{d}}}{[\text{auxin}_{\text{out}}]_{\text{d}} + K_{m1}} + \frac{k_{8b}[\text{auxin}_{\text{in}}][\text{PIN}]_{\text{d}}}{[\text{auxin}_{\text{in}}] + K_{m2}} - k_{11}[\text{auxin}_{\text{out}}]_{\text{d}} + \sum_k \{k_{ECM}[\text{auxin}_{\text{out}}]_{\text{k}}\} - \text{f}_{\text{out}}[\text{auxin}_{\text{out}}]_{\text{d}} \qquad \text{k} = b, c$$

$$\begin{aligned}\frac{d}{dt}[\text{Aux/IAA}] = {} & k_{2,x}[\text{ARF}_2/\text{DNA}] - k_3^+[\text{Aux/IAA}][\text{ARF}] + k_3^-[\text{inactive dimer}] \\ & - k_4^+[\text{Aux/IAA}][\text{ARF/DNA}] + k_4^-[\text{inactive DNA}] \\ & - k_5^+[\text{Aux/IAA}]^2 + k_5^-[(\text{Aux/IAA})_2] \\ & - \frac{k_6 K_{SCF}[\text{auxin}_{\text{in}}][\text{Aux/IAA}]}{(1 + K_{SCF}[\text{auxin}_{\text{in}}])([\text{Aux/IAA}] + K_{6m})}\end{aligned}$$

$$\frac{d}{dt}[(\text{Aux/IAA})_2] = k_5^+[\text{Aux/IAA}]^2 - k_5^-[(\text{Aux/IAA})_2]$$

$$\begin{aligned}\frac{d}{dt}[\text{ARF}] = {} & -k_1^+[\text{ARF}][\text{ARF/DNA}] + k_1^-[\text{ARF}_2/\text{DNA}] \\ & - k_3^+[\text{Aux/IAA}][\text{ARF}] + k_3^-[\text{inactive dimer}]\end{aligned}$$

$$\begin{aligned}\frac{d}{dt}[\text{ARF/DNA}] = {} & -k_1^+[\text{ARF}][\text{ARF/DNA}] + k_1^-[\text{ARF}_2/\text{DNA}] \\ & - k_4^+[\text{Aux/IAA}][\text{ARF/DNA}] + k_4^-[\text{inactive DNA}]\end{aligned}$$

$$\frac{d}{dt}[\text{ARF}_2/\text{DNA}] = k_1^+[\text{ARF}][\text{ARF/DNA}] - k_1^-[\text{ARF}_2/\text{DNA}]$$

$$\frac{d}{dt}[\text{inactive dimer}] = k_3^+[\text{Aux/IAA}][\text{ARF}] - k_3^-[\text{inactive dimer}]$$

$$\frac{d}{dt}[\text{inactive DNA}] = k_4^+[\text{Aux/IAA}][\text{ARF/DNA}] - k_4^-[\text{inactive DNA}]$$

$$\frac{d}{dt}[\text{AUX1}]_\text{j} = \frac{1}{4}\left\{k_{2,AUX}[\text{ARF}_2\text{/DNA}]\right\} - k_9[\text{AUX1}]_\text{j} \qquad \text{j} = a,b,c,d$$

$$\frac{d}{dt}[\text{PIN}]_\text{in} = k_{2,PIN}[\text{ARF}_2\text{/DNA}] - k_{10}[\text{PIN}]_\text{in} - \sum_{j=a}^{d}\left\{\frac{k_{out}[\text{PIN}]_\text{in}}{1+\left(\frac{[\text{auxin}_\text{out}]_j}{K_t}\right)^n} - k_{in}[\text{PIN}]_\text{j}\right\}$$

$$\frac{d}{dt}[\text{PIN}]_\text{j} = \frac{k_{out}[\text{PIN}]_\text{in}}{1+\left(\frac{[\text{auxin}_\text{out}]_j}{K_t}\right)^n} - k_{in}[\text{PIN}]_\text{j} \qquad \text{j} = a,b,c,d$$

Examination of these equations shows that the total concentrations of soluble ARFs and of bound DNA in the cell are constant, leading to the following conservation relations:

$$[\text{ARF}] + [\text{ARF}_2\text{/DNA}] + [\text{inactive dimer}] = a_0,$$
$$\text{and} \qquad [\text{ARF/DNA}] + [\text{ARF}_2\text{/DNA}] + [\text{inactive DNA}] = b_0.$$

Therefore, the concentrations of the inactive ARF—Aux/IAA dimers, whether free or DNA-bound, need not be tracked separately, but can be determined from the concentrations of other species:

$$[\text{inactive dimer}] = a_0 - [\text{ARF}] - [\text{ARF}_2\text{/DNA}],$$
$$\text{and} \qquad [\text{inactive DNA}] = b_0 - [\text{ARF/DNA}] - [\text{ARF}_2\text{/DNA}].$$

Chapter 3

Single-Cell Model

The differential equation model presented in Section 2.3 was simulated using the simulation software `xppaut` [162]. Several different integrators are available in `xppaut`; the (adaptive) 'stiff' integrator was used for simulations of the auxin model, because it is well suited to handle dynamics on widely varying time scales. An initial step size of $dt = 0.05$ was used, with minimum step size $dt = 1\text{x}10^{-12}$ and maximum $dt = 1$. Simulations under a variety of conditions were duplicated with other integrators (Euler, Gear, RK4) and with smaller step sizes to ensure reliability of results. This chapter describes how model parameters were chosen, simplifications made to the original model, and the results of simulations obtained using the simplified model.

3.1 Parameter Determination

After the DE system was derived, an arbitrary but biologically defensible set of parameters and initial conditions was chosen as a starting point for simulations. These parameters were then varied widely, both individually and in combination, and simulation results compared and checked for plausibility. Unfortunately, direct comparisons to experiment are difficult, because time courses – or even single-time determinations – of protein concentrations in plant cells are rarely reported. Parameter values and concentrations reported based on this model should therefore be considered as being in arbitrary units; establishing the qualitative behaviour of the model is of primary importance. If suitable quantitative data become available, model parameters could then be tuned to fit experimental time courses.

One assumption was introduced immediately to simplify the system. Auxin-mediated transcriptional regulation of both transporter genes, *AUX1* and *PIN*, is allowed in reactions (2.2). However, for all simulations the total concentration of AUX1 was set to be constant ($k_{2,AUX} = k_9 = 0$) and equally distributed between cell faces. Each parameter (with the

Table 3.1: Default parameter values for single-cell model.

Parameter	Value	Parameter	Value	Parameter	Value
f_{in}	0.1	f_{out}	1	n	1
k_{ECM}	0.01	k_{in}	1	k_{out}	2
K_t	1	k_1^+	1	k_1^-	1
$k_{2,PIN}$	2	$k_{2,AUX}$	0	$k_{2,x}$	10
k_3^+	1	k_3^-	1	k_4^+	1
k_4^-	1	k_5^+	1	k_5^-	1
k_6	0.5	k_{7b}	1	k_{8b}	1
k_9	0	k_{10}	0.005	k_{11}	0
K_{SCF}	0.1	K_{6m}	2	K_{m1}	1
K_{m2}	1	a_0	0.5	b_0	0.02

Table 3.2: Default initial conditions for single-cell model.

Species	Concentration	Species	Concentration
$auxin_{in}$	1	$auxin_{out,j}$	0
$AUX1_j$	1	PIN_{in}	1
PIN_j	0	Aux/IAA	2
$(Aux/IAA)_2$	0	ARF	0.5
ARF/DNA	0.02	ARF_2/DNA	0

exception of those involving AUX1) was then varied over several orders of magnitude, and interactions between sets of parameters were also considered. Since the model's qualitative behaviour is of interest, round values of the correct magnitude were chosen as defaults. The default parameters and initial conditions deduced from this procedure are presented in Tables 3.1 and 3.2.

3.2 Model Simplification

Upon viewing simulation results, it eventually became evident that several of the reactions included in Sections 2.1 and 2.2 had redundant effects. The model outlined there is already much simplified from reality. Nevertheless, less complex systems are easier to study, and so any simplifications that preserve the core behaviours of the model are, in general, desirable.

A key part of auxin signalling is the inhibition of transcription by Aux/IAA proteins. Two possible methods of inhibition are included in reactions (2.3): Aux/IAAs may titrate out free ARFs, or they may physically impede ARF dimerization on DNA promoters [163]. Either mechanism leads to fewer ARFs that are able to dimerize and promote transcription of auxin-responsive genes. Simulations were carred out using each of the inhibition mechanisms separately, and it was found that there were only quantitative differences from the case where both are included simultaneously. (Compare Figure 3.1a,b with 3.1c,d.) Since Aux/IAAs are directly involved in the reaction that is being 'turned off', their initial behaviour differs somewhat, but the traces can be made essentially identical by altering other parameter values slightly. The model used in all subsequent sections therefore includes Aux/IAAs interacting only with free ARFs (*i.e.*, $k_4^+ = k_4^- = 0$).

Another simplification is warranted by lack of knowledge about the experimental system. The dimerization of Aux/IAA proteins postulated in reaction 2.4 is certainly possible, but the extent and/or importance of this feature *in vivo* is unknown [105, 133]. As above, simulations performed with and without reaction 2.4 gave qualitatively similar results. (Compare Figure 3.1a,b with 3.1e,f.) Aux/IAA homodimerization was therefore omitted from the model for all subsequent simulations (*i.e.*, $k_5^+ = k_5^- = 0$). Future revisions of the auxin model may include multiple Aux/IAAs, among which various differences have been amply demonstrated [134, 164, 165]. Also, there seem to be some differences (such as the involvement of domain I, not just domain III) between homodimerization and heterodimerization of Aux/IAAs [166]. Therefore, if multiple Aux/IAA species were to be

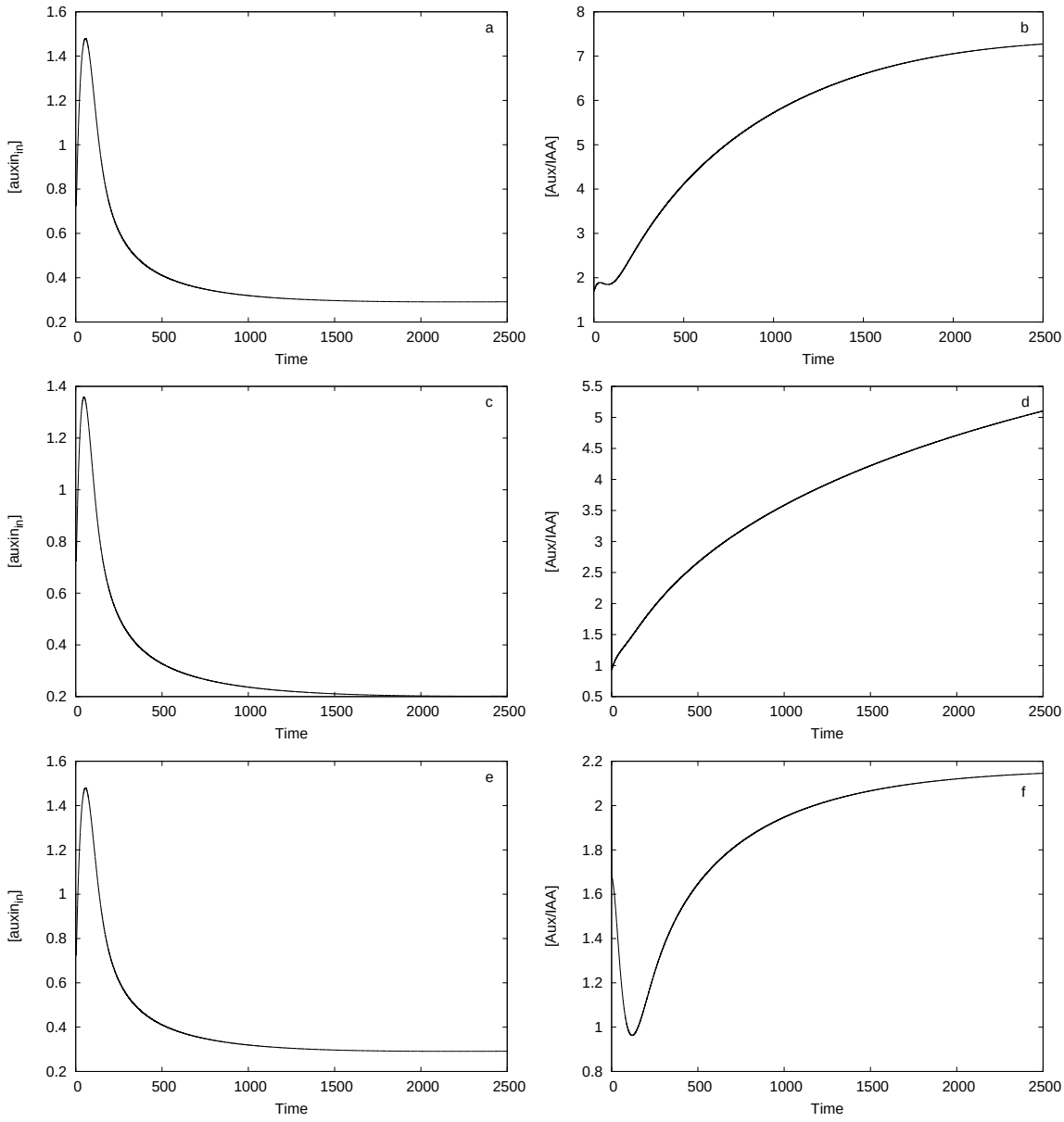

Figure 3.1: Comparison of original and simplified models. Time courses of internal IAA (a,c,e,g) and Aux/IAA (b,d,f,h) concentrations. (a,b) Original model, with all parameters as in Table 3.1. (c,d) Without Aux/IAA binding to ARF/DNA ($k_4^+ = k_4^- = 0$). (e,f) Without Aux/IAA homodimerization ($k_5^+ = k_5^- = 0$). (g,h) See page 27.

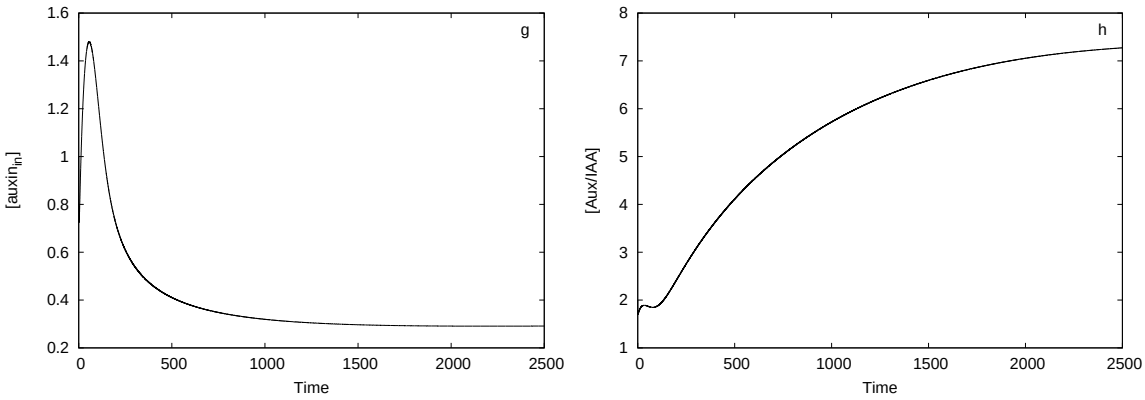

Figure 3.1: Continued from page 26. (g,h) Simplified model ($k_4^+ = k_4^- = k_5^+ = k_5^- = 0$). Note similarity to original behaviour in (a,b).

considered in the course of further investigations, a suitably modified version of reaction 2.4 would likely assume greater importance.

3.3 Simplified Model Equations

The omission of Aux/IAA—ARF/DNA interaction and of Aux/IAA homodimerization means that any rate equations involving those processes must be modified. The DE system corresponding to the simplified system is presented below (see also Figure 3.1(g,h)). Essentially, it is the result of setting $k_4^+ = k_4^- = k_5^+ = k_5^- = 0$ in the equations of Section 2.3. It is this set of DEs that was used as the basis for all simulations in the remainder of this thesis. A schematic of the auxin system is given in Figure 3.2.

$$\frac{d}{dt}[\text{auxin}_{\text{in}}] = \sum_{j=a}^{d}\left\{\frac{k_{7b}[\text{AUX1}]_{\text{j}}[\text{auxin}_{\text{out}}]_{\text{j}}}{[\text{auxin}_{\text{out}}]_{\text{j}}+K_{m1}} - \frac{k_{8b}[\text{PIN}]_{\text{j}}[\text{auxin}_{\text{in}}]}{[\text{auxin}_{\text{in}}]+K_{m2}} + k_{11}[\text{auxin}_{\text{out}}]_{\text{j}}\right\}$$

$$\frac{d}{dt}[\text{auxin}_{\text{out}}]_{\text{a}} = \text{f}_{\text{in}} - \frac{k_{7b}[\text{auxin}_{\text{out}}]_{\text{a}}[\text{AUX1}]_{\text{a}}}{[\text{auxin}_{\text{out}}]_{\text{a}}+K_{m1}} + \frac{k_{8b}[\text{auxin}_{\text{in}}][\text{PIN}]_{\text{a}}}{[\text{auxin}_{\text{in}}]+K_{m2}} - k_{11}[\text{auxin}_{\text{out}}]_{\text{a}} + \sum_{k}\{k_{ECM}[\text{auxin}_{\text{out}}]_{\text{k}}\} \qquad \text{k} = \text{b},\text{c}$$

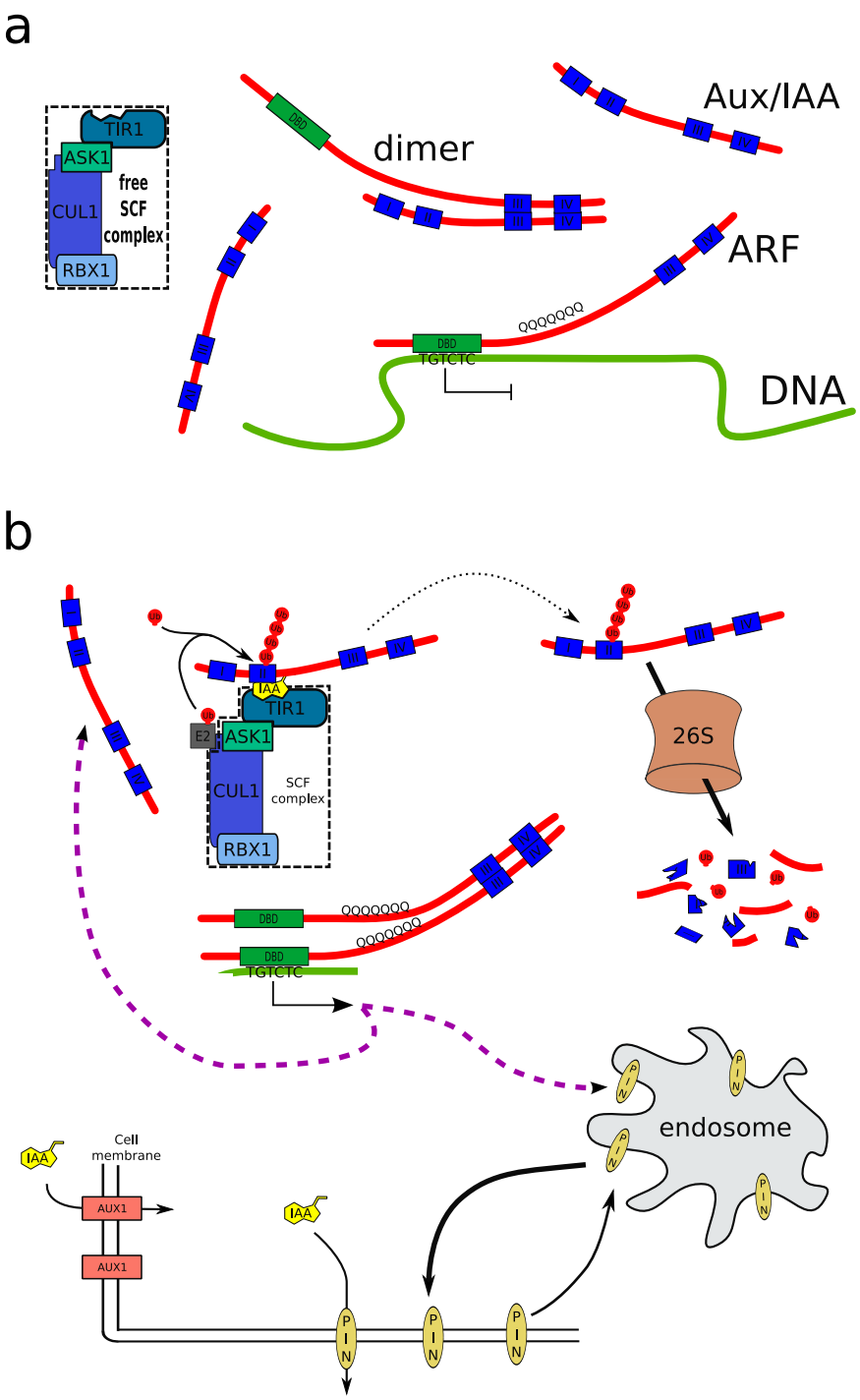

Figure 3.2: Schematic of the auxin signalling system. (a) No auxin present. Aux/IAA repressors bind to ARF transcription factors, preventing ARF dimerization on auxin-responsive DNA elements (AuxREs; TGTCTC motif) and thereby inhibiting transcription. (b) With auxin present. Auxin enables the interaction of SCF^{TIR1} with Aux/IAAs, leading to their ubiquitination and subsequent degradation by the 26S proteasome. In the absence of Aux/IAAs, ARFs homodimerize on AuxREs and transcription of PINs and of Aux/IAAs commences.

$$\frac{d}{dt}[\text{auxin}_{\text{out}}]_{\text{j}} = -\frac{k_{7b}[\text{auxin}_{\text{out}}]_{\text{j}}[\text{AUX1}]_{\text{j}}}{[\text{auxin}_{\text{out}}]_{\text{j}}+K_{m1}} + \frac{k_{8b}[\text{auxin}_{\text{in}}][\text{PIN}]_{\text{j}}}{[\text{auxin}_{\text{in}}]+K_{m2}} - k_{11}[\text{auxin}_{\text{out}}]_{\text{j}} + \sum_k \{k_{ECM}[\text{auxin}_{\text{out}}]_{\text{k}}\} \qquad \text{j} = \text{b,c};\ \text{k} = \text{neighbours}$$

$$\frac{d}{dt}[\text{auxin}_{\text{out}}]_{\text{d}} = -\frac{k_{7b}[\text{auxin}_{\text{out}}]_{\text{d}}[\text{AUX1}]_{\text{d}}}{[\text{auxin}_{\text{out}}]_{\text{d}}+K_{m1}} + \frac{k_{8b}[\text{auxin}_{\text{in}}][\text{PIN}]_{\text{d}}}{[\text{auxin}_{\text{in}}]+K_{m2}} - k_{11}[\text{auxin}_{\text{out}}]_{\text{d}} + \sum_k \{k_{ECM}[\text{auxin}_{\text{out}}]_{\text{k}}\} - \text{f}_{\text{out}}[\text{auxin}_{\text{out}}]_{\text{d}} \qquad \text{k} = \text{b,c}$$

$$\frac{d}{dt}[\text{Aux/IAA}] = k_{2,x}[\text{ARF}_2/\text{DNA}] - k_3^+[\text{Aux/IAA}][\text{ARF}] + k_3^-[\text{inactive dimer}] - \frac{k_6 K_{SCF}[\text{auxin}_{\text{in}}][\text{Aux/IAA}]}{(1+K_{SCF}[\text{auxin}_{\text{in}}])([\text{Aux/IAA}]+K_{6m})}$$

$$\frac{d}{dt}[\text{ARF}] = -k_1^+[\text{ARF}][\text{ARF/DNA}] + k_1^-[\text{ARF}_2/\text{DNA}] - k_3^+[\text{Aux/IAA}][\text{ARF}] + k_3^-[\text{inactive dimer}]$$

$$\frac{d}{dt}[\text{ARF/DNA}] = -k_1^+[\text{ARF}][\text{ARF/DNA}] + k_1^-[\text{ARF}_2/\text{DNA}]$$

$$\frac{d}{dt}[\text{ARF}_2/\text{DNA}] = k_1^+[\text{ARF}][\text{ARF/DNA}] - k_1^-[\text{ARF}_2/\text{DNA}]$$

$$\frac{d}{dt}[\text{inactive dimer}] = k_3^+[\text{Aux/IAA}][\text{ARF}] - k_3^-[\text{inactive dimer}]$$

$$\frac{d}{dt}[\text{AUX1}]_{\text{j}} = \frac{1}{4}\left\{k_{2,AUX}[\text{ARF}_2/\text{DNA}]\right\} - k_9[\text{AUX1}]_{\text{j}} \qquad \text{j} = \text{a,b,c,d}$$

$$\frac{d}{dt}[\text{PIN}]_{\text{in}} = k_{2,PIN}[\text{ARF}_2/\text{DNA}] - k_{10}[\text{PIN}]_{\text{in}} - \sum_{j=a}^{d}\left\{\frac{k_{out}[\text{PIN}]_{\text{in}}}{1+\left(\frac{[\text{auxin}_{\text{out}}]_j}{K_t}\right)^n} - k_{in}[\text{PIN}]_{\text{j}}\right\}$$

$$\frac{d}{dt}[\mathrm{PIN}]_\mathrm{j} = \frac{k_{out}[\mathrm{PIN}]_\mathrm{in}}{1+\left(\frac{[\mathrm{auxin_{out}}]_j}{K_t}\right)^n} - k_{in}[\mathrm{PIN}]_\mathrm{j} \qquad \mathrm{j} = \mathrm{a,b,c,d}$$

The resulting conservation relations are slightly different than those in Section 2.3:

$$\begin{aligned}[\mathrm{ARF}] + [\mathrm{ARF_2/DNA}] + [\text{inactive dimer}] &= a_0, \\ \text{and} \qquad [\mathrm{ARF/DNA}] + [\mathrm{ARF_2/DNA}] &= b_0.\end{aligned}$$

Again, the conservation expressions allow the concentration of inactive ARF—Aux/IAA dimers and of DNA-bound ARFs to be determined from those of other species:

$$\begin{aligned}[\text{inactive dimer}] &= a_0 - b_0 - ([\mathrm{ARF}] - [\mathrm{ARF/DNA}]), \\ \text{and} \qquad [\mathrm{ARF_2/DNA}] &= b_0 - [\mathrm{ARF/DNA}]).\end{aligned}$$

3.4 PIN Production & Competition Models

In addition to redistribution of PINs, an obvious way for a cell to respond to increasing auxin levels is to produce more of the efflux transporters. While PINs were not originally identified as auxin-responsive gene products [167], their transcription has since been shown to increase in an auxin-dependent manner [168]. PIN production was therefore included in reactions (2.2), though at a lower rate than for Aux/IAAs, which are primary auxin response products. According to results reported by Geldner *et al.*, however, PINs are not significantly turned over except on quite long time scales [155]. An alternative version of the model was therefore constructed, which maintains a constant total PIN level (by setting $k_{2,PIN} = k_{10} = 0$, as was done for AUX1 in Section 3.1). In this situation, cell faces must

Table 3.3: Default parameter values for PIN production and competition models. Parameters shown here are only those that differ between the two models, or from the default parameters in Table 3.1.

Parameter	Production	Competition	Parameter	Production	Competition
$k_{2,PIN}$	2	0	k_{10}	0.005	0
f_{in}	0.5	0.5	f_{out}	1	1

compete for a limited number of PIN transporters, and this is termed the 'competition' model. The original version, with additional PINs produced in response to auxin, is called the 'production' model. Default values for those parameters that differ between the two model versions are summarized in Table 3.3, as well as the auxin flow parameters used for simulations with both. All other parameters retain their default values in both model versions (Table 3.1), and in both model versions PINs are able to cycle between cell faces and an internal pool.

For consistency, all simulations depicted in the remainder of this thesis were started from a low-auxin equilibrium. This state was obtained by starting with an internal auxin concentration of 0.1 units, and no external auxin. The closed system (no auxin influx or efflux; $f_{in} = f_{out} = 0$) was then simulated with all parameters at default values until equilibrium was reached ($t = 100\,000$ for PIN production model, $t = 200\,000$ for PIN competition model). The resulting equilibrium concentrations are summarized in Table 3.4, and were used as initial conditions for all subsequent simulations.

3.5 Auxin Flow Simulations

As described in the previous section, two possibilities were considered for PIN response to auxin: the 'production' model (PINs are produced in response to auxin), and the 'competition' model (total PIN concentration is held constant). As expected, the two versions of

Table 3.4: Initial conditions for PIN production and competition model simulations, representing low-auxin equilibrium. These initial conditions were obtained by simulating models using default parameters (Tables 3.1 and 3.3) and initial conditions (Table 3.2) until equilibrium was reached, as described in the text.

Species	Production	Competition	Species	Production	Competition
$[\text{auxin}_{\text{in}}]$	0.0561	0.0274	$[\text{auxin}_{\text{out}}]_{\text{j}}$	0.0112	0.0181
$[\text{AUX1}]_{\text{j}}$	1	1	$[\text{PIN}]_{\text{in}}$	0.1057	0.3387
$[\text{PIN}]_{\text{j}}$	0.2091	0.6653	$[\text{Aux/IAA}]$	36.32	71.65
$[\text{ARF}]$	0.0134	0.0069	$[\text{ARF/DNA}]$	0.0112	0.0199

the model exhibit marked differences in their responses to the onset of auxin flow. Figure 3.3 depicts the results of initiating top-to-bottom auxin flow through a model cell initially at low-auxin equilibrium (*i.e.*, at the initial conditions shown in Table 3.4). In the production model, a low initial PIN concentration means that auxin entering the cell cannot be efficiently exported, and the internal auxin concentration initially increases rapidly (Fig. 3.3a). By contrast, in the competition model, there is immediately enough PIN protein present to efficiently remove auxin, and thus the internal auxin concentration only slowly rises to its eventual level (Fig. 3.3b). The production model does also eventually attain a stable internal auxin concentration, after enough PIN has been produced to keep up with the influx of auxin (Fig. 3.3c).

In both the PIN production and competition models, the final external concentration of auxin on each side of the cell is very similar (Fig. 3.3d,e). Interestingly, though, the equilibrium concentrations of auxin inside the cell differ significantly, as may be seen by comparing Figure 3.3a to 3.3b. The PIN production model with sustained auxin flow has an internal auxin concentration significantly lower than that above the cell (and even somewhat lower than is found on cell sides *b* and *c*; Fig. 3.3a,d). In the PIN competition scenario, by

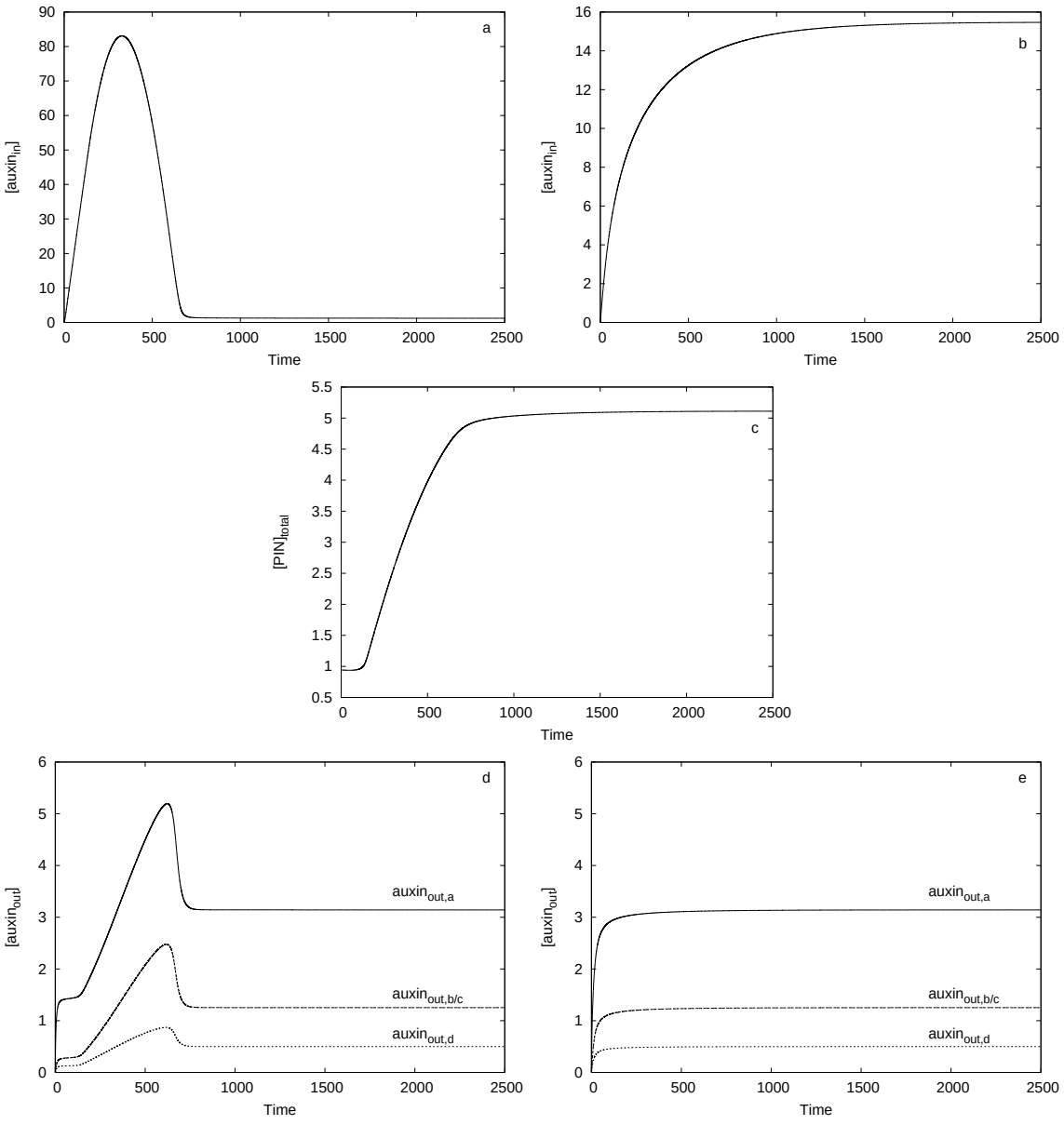

Figure 3.3: Comparison of auxin levels in PIN production & competition models; all parameters at default values. PIN production model in (a,c,d); PIN competition model in (b,e). (a,b) Internal auxin concentration time courses. (c) Total PIN concentration time course. (d,e) External auxin concentration time courses.

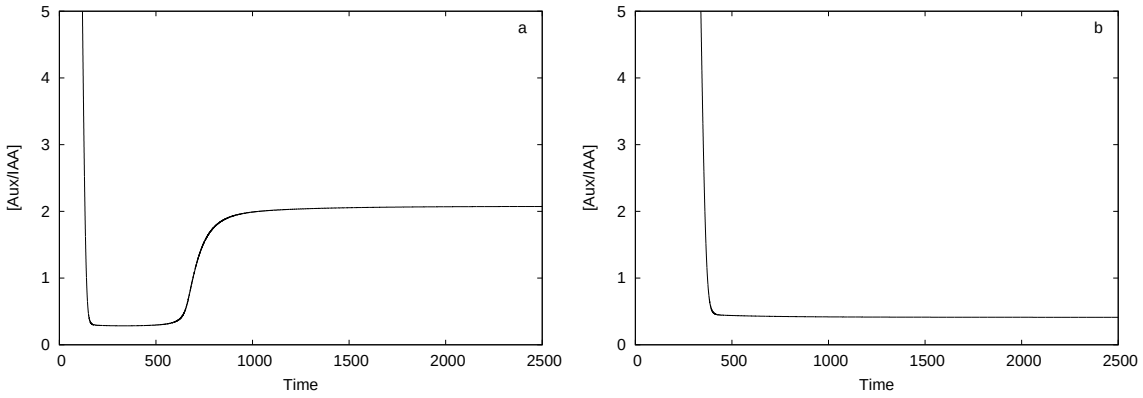

Figure 3.4: Comparison of Aux/IAA concentration time courses in PIN production & competition models. All parameters set to default values. (a) PIN production model. (b) PIN competition model.

contrast, the internal auxin concentration is much higher than the concentration outside the cell (Fig. 3.3b,e). The possible significance of this difference is discussed in Chapter 5.

In addition to auxin levels, the concentration of Aux/IAA signalling molecules differs between the two model versions (Fig. 3.4a,b). In the PIN production model, Aux/IAAs are degraded while the internal auxin level remains high. Once most of the auxin has been expelled from the cell by newly manufactured PINs, fewer Aux/IAAs are degraded than are produced, and the concentration rebounds (Fig. 3.4a). This is consistent with initial descriptions of Aux/IAAs as rapid auxin-responsive gene products [123, 169], increasing in concentration some minutes after auxin application. In the PIN competition case, the much higher equilibrium concentration of internal auxin induces continued Aux/IAA degradation; as a result, Aux/IAA concentrations remain low (Fig. 3.4b).

One drawback of the PIN competition model is its greater sensitivity to changing parameter values. If the rate of auxin addition is increased beyond that used in the simulations above, the PIN production model compensates by producing more PIN proteins; though it takes longer, eventually a stable equilibrium is still reached (Fig. 3.5a; compare Fig. 3.3a). In the PIN competition model, though, the total amount of PIN is fixed; increasing the auxin influx to $f_{in} = 1$ (with all other parameters unchanged), causes the obviously unphys-

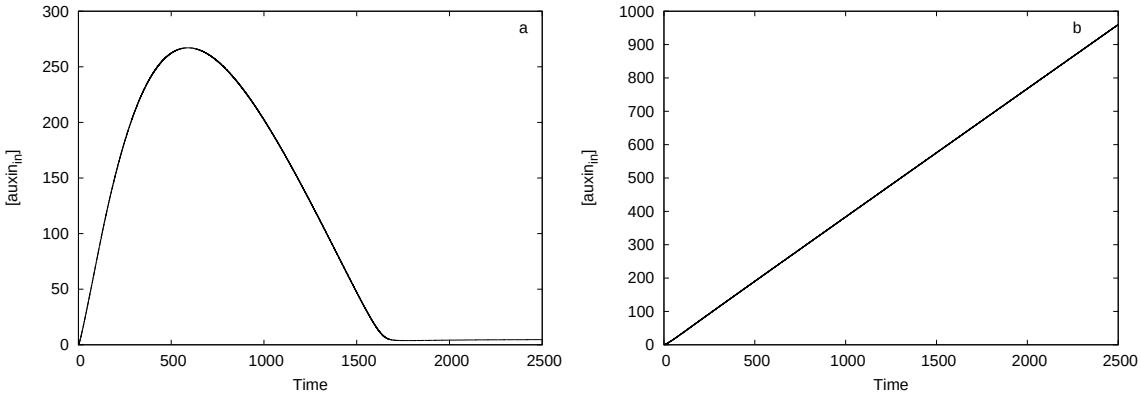

Figure 3.5: Comparison of PIN production & competition model responses to high auxin flow. Model parameters as in Figure 3.3, except $f_{in} = 1$. (a) PIN production model. (b) PIN competition model.

ical situation of a constantly increasing internal auxin concentration, shown in Figure 3.5b. Within real plants, auxin homeostasis mechanisms not included in our model would likely be engaged to cope with such accumulation. In our model, of course, the initial amount of PIN in the competition case could be artificially adjusted as necessary to compensate for higher auxin influx, but the PIN production model is able to cope without such undesirable manipulation. In reality, the PIN competition and production models introduce a false dichotomy; a hybrid of the two is more likely to operate. Competition for existing PINs would provide the fast initial response to auxin, while production of more PINs would follow and enable a slower adaptation to a sustained auxin presence.

In both model versions, the distribution of PIN proteins among the sides of the cell is key to auxin transport; the localization of PINs is the mechanism by which transport polarity is determined. The response of cellular PIN distribution to different levels of auxin flow was examined. As expected, PINs are evenly distributed among cell sides in the absence of auxin flow (Fig. 3.6a). As the flow of auxin from the top to bottom of the cell is increased, the PIN proteins become more and more asymmetrically localized (Fig. 3.6b,c). Interestingly, the proportion of PIN proteins on each cell face is the same in both the PIN

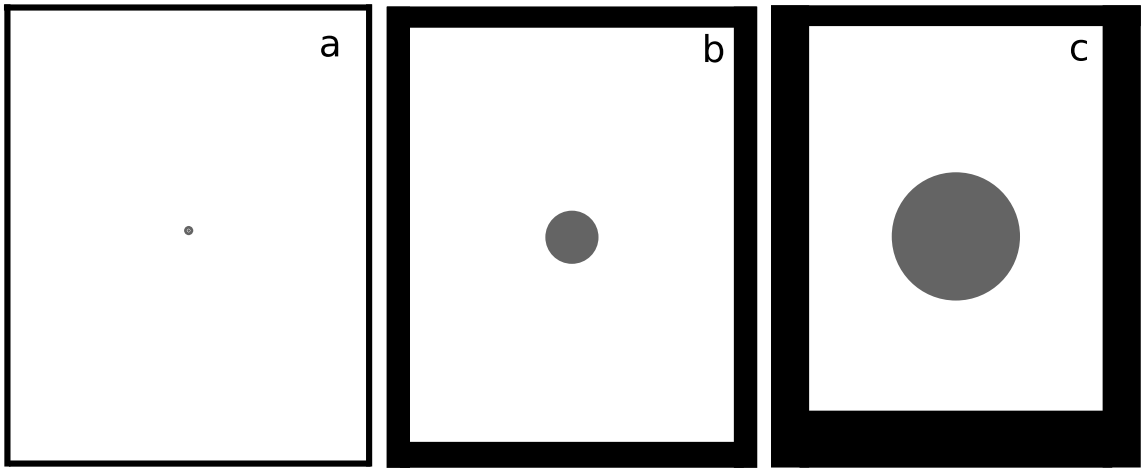

Figure 3.6: Polar PIN redistribution in response to auxin flow. All parameters at default values unless otherwise noted. Line weights (and circle diameter) are proportional to relative concentrations of PIN proteins at each face (and in the internal endosomal pool). Weights shown are for the PIN production model; results for the competition model are similar, but have lower absolute PIN concentrations and higher internal auxin levels. (a) Low-auxin equilibrium ($f_{in} = f_{out} = 0$). (b) Low auxin flow from top to bottom ($f_{in} = 0.1$, $f_{out} = 1$). (c) Moderate auxin flow ($f_{in} = 0.5$, $f_{out} = 1$; *i.e.*, default conditions, as used in previous figures).

competition and production models, despite (sometimes large) differences between absolute PIN concentrations.

3.6 Auxin Pulse Simulations

PIN redistribution and other cellular events examined here occur very early after auxin application. Externally visible changes such as cell polarization [170] and tracheary element formation [171–173] occur at much later stages, and imply an irreversible commitment to vascular cell fate. It is likely, however, that a commitment to vascular cell identity is made at a growth stage well before gross morphological changes occur. In particular, it is possible that a sufficiently large change in the PIN redistribution system modelled here could cause the cell to 'switch' fates and adopt a stable auxin transport direction. The polarity induced by different levels of steady auxin flow through the cell, treated in Section 3.5, is stable only as long as the flow was continued. The response of model cells to pulses

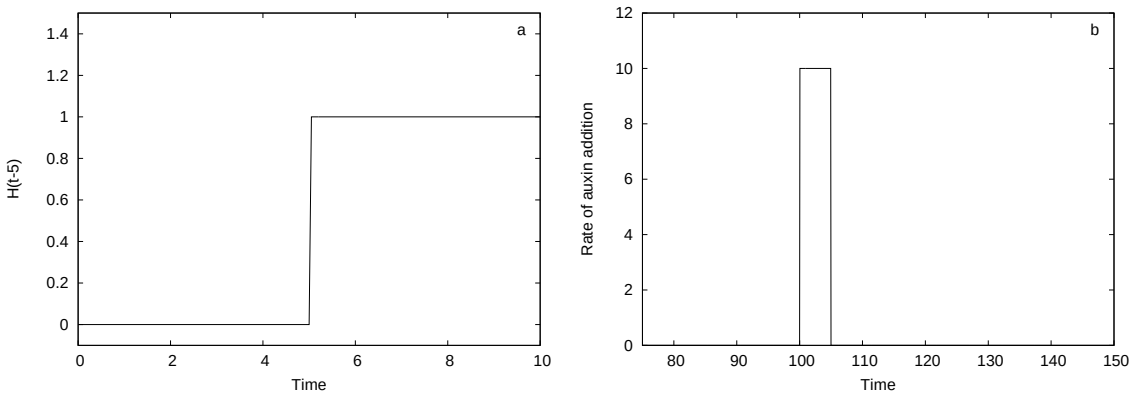

Figure 3.7: (a) Heaviside function, $f(t) = H(\mathrm{t}-5)$. $f(t) = 0$ for $\mathrm{t} < 5$, and $f(t) = 1$ for $\mathrm{t} < 5$ (b) Diagram of an auxin pulse. Here $\mathrm{p_{size}} = 10$, $\mathrm{p_i} = 100$ and $\mathrm{p_f} = 105$, so auxin is added to the extracellular space above the cell at a rate of 10 (units of $\frac{\text{concentration}}{\text{time}}$) from $\mathrm{t} = 100$ until $\mathrm{t} = 105$.

(brief, intense applications) of auxin was therefore examined to investigate whether such a mechanism could be sufficient to cause permanent cell polarization [40].

Simulations were run under the same conditions as in Figure 3.3 to facilitate comparisons, and allowed to proceed until equilibrium was reached ($\mathrm{t} = 5000$). Auxin pulse simulations were then begun from that equilibrium condition. Additional external auxin is supplied by increasing the amount of auxin influx from above the cell for a specified period, using the Heaviside step function built into `xppaut` (Heaviside function $H(\mathrm{t}-\mathrm{a})$ has value 0 for $\mathrm{t} < \mathrm{a}$ and value 1 for $\mathrm{t} > \mathrm{a}$; Fig. 3.7a). The result is a slightly modified version of the DE for $[\mathrm{auxin_{out}}]_\mathrm{a}$:

$$\begin{aligned}\frac{d}{dt}[\mathrm{auxin_{out}}]_\mathrm{a} &= \mathrm{f_{in}} + \mathrm{p_{size}}\Big(H(\mathrm{t}-\mathrm{p_i}) - H(\mathrm{t}-\mathrm{p_f})\Big) \\ &\quad - \frac{k_{7b}[\mathrm{auxin_{out}}]_\mathrm{a}[\mathrm{AUX1}]_\mathrm{a}}{[\mathrm{auxin_{out}}]_\mathrm{a} + K_{m1}} + \frac{k_{8b}[\mathrm{auxin_{in}}][\mathrm{PIN}]_\mathrm{a}}{[\mathrm{auxin_{in}}] + K_{m2}} \\ &\quad - k_{11}[\mathrm{auxin_{out}}]_\mathrm{a} + \sum_{k=b,c}\{k_{ECM}[\mathrm{auxin_{out}}]_\mathrm{k}\},\end{aligned}$$

where new parameters $\mathrm{p_{size}}$, $\mathrm{p_i}$ and $\mathrm{p_f}$ are the magnitude, starting and ending times, respectively, of the auxin pulse application. Figure 3.7b shows a diagrammatic view of an auxin pulse.

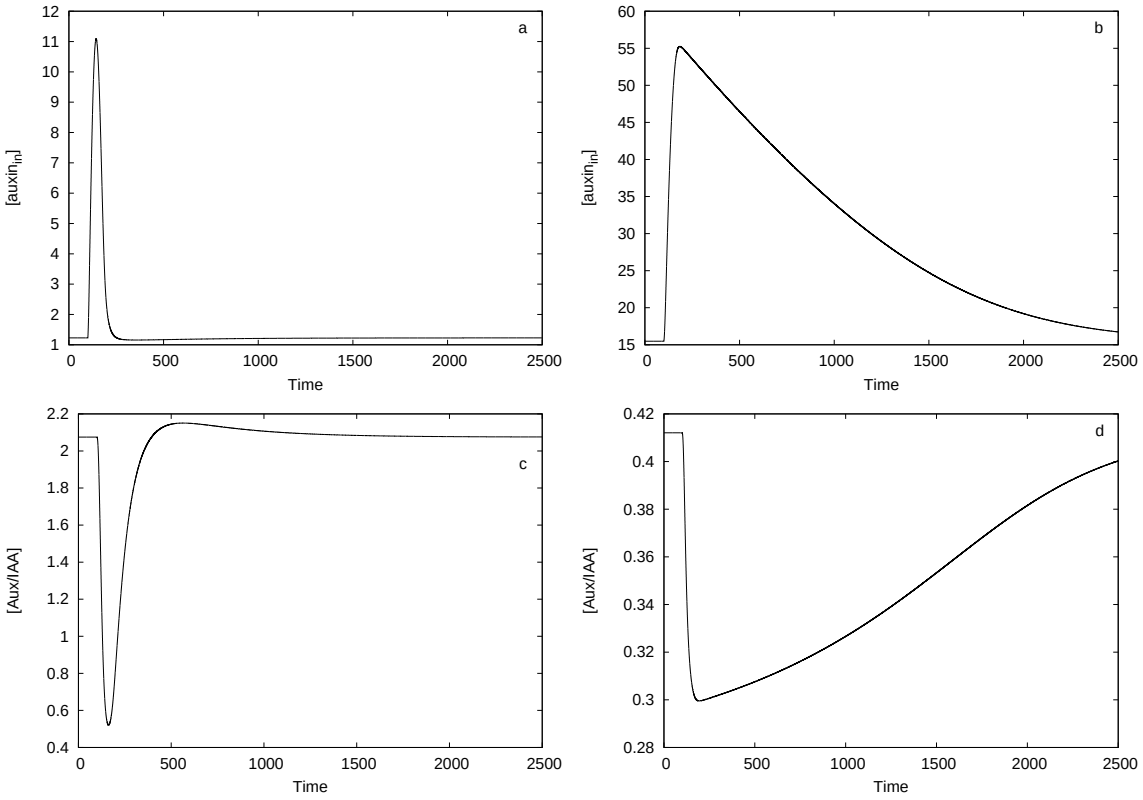

Figure 3.8: Cell response to auxin pulse application (additional influx rate=10, applied from t=100 to t=105, after equilibration at the conditions of Figure 3.3). PIN production model in (a,c); PIN competition model in (b,d). (a,b) Internal auxin time courses. (c,d) Aux/IAA time courses.

Simulation results with auxin pulses are depicted in Figures 3.8 and 3.9. As seen in Figure 3.8a,b, internal auxin does accumulate rapidly upon auxin application, as expected. However, this accumulation is temporary, and the final internal auxin concentration is unchanged from the constant-flow situation with no pulse applied (compare Fig. 3.3), in both the PIN production and competition cases. The same is true for Aux/IAAs (Fig. 3.8c,d) and PIN proteins (Fig. 3.9). The Aux/IAA concentration can be clearly seen to be diminished by auxin-induced degradation, and then to be produced in response to auxin signalling and return to its previous level. Similarly, the distribution of PINs changes dramatically to accomodate the additional auxin above the cell, but as soon as the pulse of auxin has beendealt with, the system reverts to the state in which it was prior to the pulse.

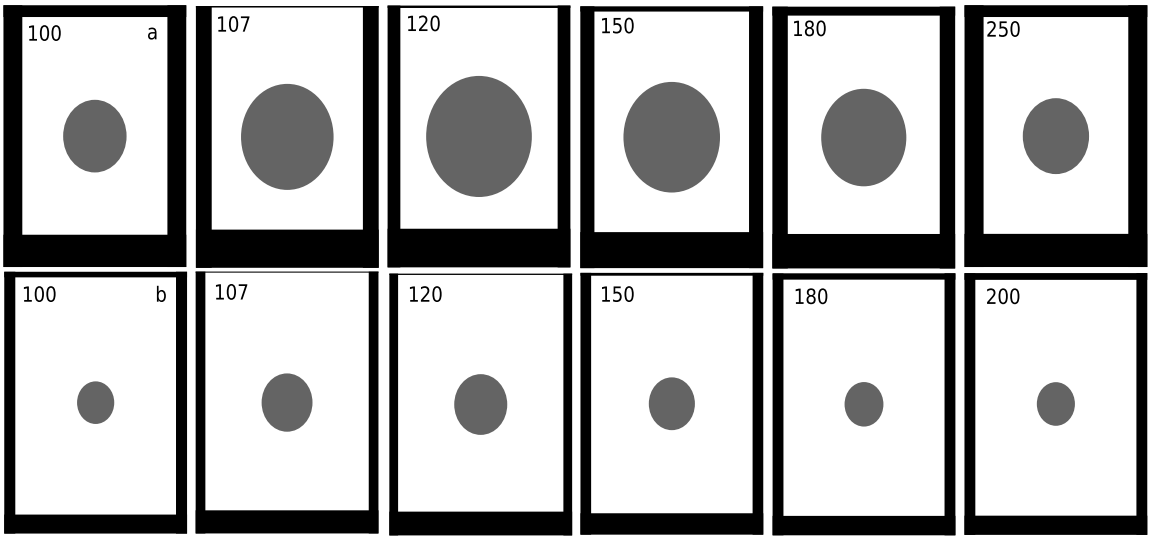

Figure 3.9: Polar PIN redistribution at cell faces in response to auxin pulse application; conditions as in Figure 3.8. Line weights (and circle diameter) are proportional to relative concentrations of PIN proteins at each face (and in the internal endosomal pool). Times are in top left corner. (a) PIN production model. (b) PIN competition model.

The same phenomenon occurs with only minor variations if the auxin pulse is administered at different times, from another direction than the steady flow, with no additional flow at all, or if the pulse is larger or replaced by multiple (simultaneous or sequential) pulses [data not shown]. In many of these enumerated cases the only difference from the simulations shown is in the time that the system takes to return to its original state. If instead of a transient pulse a permanently higher level of auxin flow is introduced, the cell (as expected) becomes more highly polarized (Fig. 3.10). But this change, too, is not permanent; reducing auxin flow again restores the same internal conditions. These results suggest that the auxin relocation mechanism modelled here, while it is highly plastic, is not sufficient in isolation to develop permanent cellular polarization of auxin transport. Instead, the equilibrium state adopted by the modelled cell depends only on the permanent auxin flow through the cell.

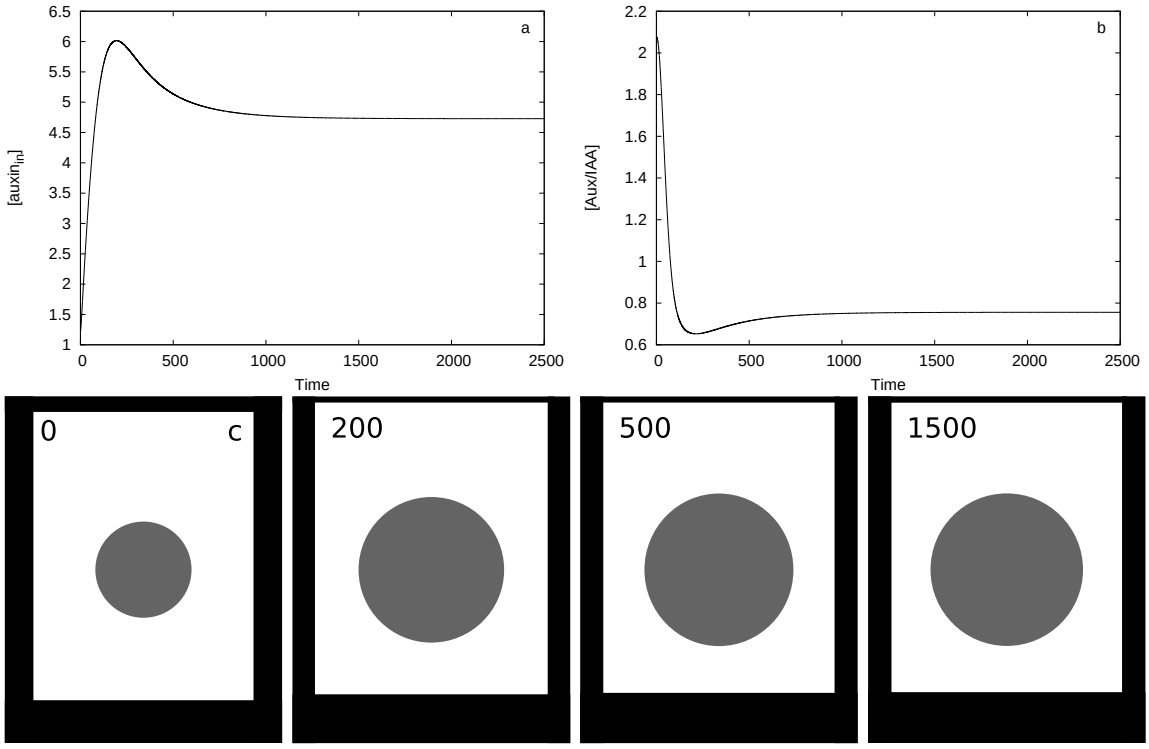

Figure 3.10: Cell response to increased auxin influx in the PIN production model ($f_{in} = 1.0$, after equilibration at the conditions of Figure 3.3). (a) Internal auxin time course. (b) Aux/IAA time course. (c) Polar PIN redistribution. Line weights (and circle diameter) are proportional to relative concentrations of PIN proteins at each face (and in the internal endosomal pool). Times are in top left corner.

3.7 PIN Targeting

The cellular mechanisms for auxin's control of transporter targeting remain largely unknown. The PINOID (PID) kinase is at least partially responsible [150, 170, 174, 175]. Different types of PIN proteins also affect each other and are partially functionally redundant, even showing unusual polarity if required to compensate for missing transporters [63, 64, 176–178]. The signalling involved in this replacement seems to depend on the *PLETHORA* (*PLT*) genes [176, 179]. Different PINs have different targeting pathways, too, though; PIN1 is controlled by GNOM, while PIN2 and others are independent of GNOM control [156, 180, 181].

The model developed in Chapter 2 posits a feedback from extracellular auxin concentration to PIN targeting, but leaves the mechanism unspecified. Equation 2.8 describes the targeting of PINs to cell membranes on the basis of external auxin concentration. The form of this targeting – an important feedback from auxin to the control of its transport – can be changed by altering the parameter n, set equal to 1 for all simulations described thus far. Simulations with various values of n can be seen in Figure 3.11. Larger values of n provide a steeper response around the threshold (K_t), and typically more polarized cells.

In several other models of auxin transport [65, 101], PINs are localized towards cell faces with higher external auxin concentrations, instead of lower. Such behaviour can be reproduced by allowing negative values for n, corresponding to switching the bias of PIN targeting (Fig. 3.11d,h). The single-cell model developed here is thus quite flexible; of interest will be the effects of changing n in multicell simulations.

It should be noted that despite the high degree of nonlinearity introduced by positing higher values for exponent n, no indication of permanent cell polarization is seen. The conclusion reached in the previous section therefore remains valid: the modelled portion of the auxin system is insufficient to determine permanent cell fate, at least under the conditions so far considered.

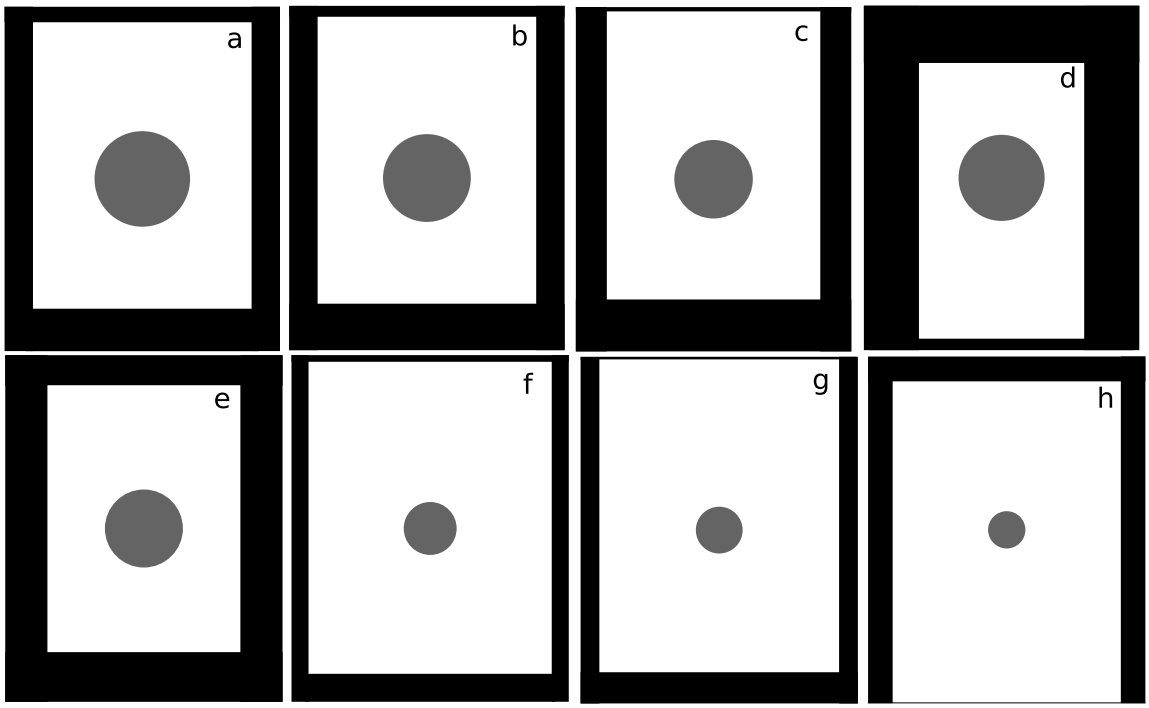

Figure 3.11: PIN localization under differing hypotheses for PIN polarity determination. Line weights (and circle diameter) are proportional to relative concentrations of PIN proteins at each face (and in the internal endosomal pool). All parameters at default values except as noted. (a-e) PIN production model, (f-h) PIN competition model. (a,e) $n = 1$ (default, as in Fig 3.6c); in (e), $K_t = 10$. (b,f) $n = 2$. (c,g) $n = 10$. (d,h) $n = -2$.

Chapter 4

Multicell Model

Pattern formation does not happen, of course, within a single cell, although the dynamics of single cells underlie the phenomena observed in larger tissues. The model of auxin signalling and transport regulation developed in the previous chapters was therefore extended to a two-dimensional array of cells representing, for instance, a layer of undifferentiated subepidermal tissue in a leaf primordium. This array, called simply a 'leaf' for convenience, is composed of individual cells each instantiating the reaction dynamics laid out in Section 3.3. The cells communicate indirectly through the transport of auxin.

4.1 Model Setup & Parameters

Cellular auxin is exported (by PIN proteins) to and imported (by AUX1 transporters) from the adjoining extracellular space, not directly to and from neighbouring cells (Eqns. (2.6)). The concentrations of auxin in the extracellular matrix[1] (ECM) on sides j of a cell are therefore variables ($[\text{auxin}_{\text{out}}]_j$) to be considered along with the concentrations of various species within the (presumably well-mixed) cell. Every region of the ECM is shared by two cells (Fig. 2.1), so $[\text{auxin}_{\text{out}}]_a$ of a given non-edge cell is identified with $[\text{auxin}_{\text{out}}]_d$ of the cell above, and similarly $[\text{auxin}_{\text{out}}]_b$ of each interior cell is identical to $[\text{auxin}_{\text{out}}]_c$ of the cell directly to the left. Each region of the ECM is assumed to be rapidly mixed, and to therefore have a uniform concentration of auxin. Cells on the margins of the leaf have no extracellular space and no possibility of transport towards the outside of the leaf (except for petiole cells; see below).

Cells are laid out in a rectangular grid for convenience. The default dimensions chosen are a 19 x 19 array of cells. This is fairly small for ease of simulation, and has an odd number of columns so that there is a central cell file. The exact size is arbitrarily chosen,

[1] Extracellular matrix is used here to mean everything between the cell membranes of two neighbouring cells – *i.e.*, the cell walls and the middle lamella.

Table 4.1: Default parameter values for multicell model

Parameter	Value	Parameter	Value	Parameter	Value
N_{cols}	19	N_{rows}	19	$prod_b$	0.0
width	1	prod	2.0	p_{width}	1

but is not unrealistic for the stage of primordium formation during which the very earliest auxin transport-mediated patterning occurs [15, 16, 182]. Assuming the modelled 'leaf' to correspond to this early primordium, an influx of auxin would be expected from the epidermal convergence point (CP) at the tip of the leaf. This is modelled by allowing auxin production in a number (parameter 'width') of cells in the center of the top row of cells at a given rate ('prod') that is analogous to the parameter f_{in} in the single cell model. (Note, though, that this specific auxin production occurs in only one or a few cells, corresponding to the internalization of epidermal auxin flow at the tip CP.) The multicell equivalent to the single-cell parameter f_{out} is somewhat less exact. The leaf primordium is attached to the stem by a petiole which is assumed to connect to a sink in the form of stem vasculature. The model accounts for this by allowing efflux in a basal direction from a number ('p_{width}') of cells in the center of the bottom row. Auxin reaching the petiole is assumed to be removed by existing stem vasculature, and cannot re-enter the leaf. The default width for both source (epidermal CP) and sink (petiole) is one cell (Table 4.1). A basal auxin production rate ('$prod_b$') in all cells is also allowed, though set to zero by default.

A summary of default parameter values used in multicell simulations is presented in Table 4.1. Multicell simulations were carried out with C++, using the Roussels' first-order (adaptive) Gear integrator [183] with a default step size $dt = 0.0125$.

4.2 Simulation Results

A full exploration of parameter space in the multicell model has not yet been performed. This section will describe the results of simulations at selected parameter values, as an indication of the model's performance and possible applications. An obvious place to start is with the same default parameters and conditions as were used in the single-cell model. Results of multicell simulations for 500 time units at the original default values (Tables 3.1 and 3.2) and at the default values for the PIN production model (Tables 3.3 and 3.4) are illustrated in Figures 4.1 and 4.2, respectively. Apart from a few differences in detail, these simulations and those using the default initial conditions from the PIN competition model [not shown] behave similarly. Auxin produced specifically at the top of the leaf rapidly dissipates, and auxin concentrations form a gradient from top to bottom of the leaf. There is some evidence of sink-driven formation of a central region of cells with noticeably lower auxin concentration than its neighbours.

Because no internal PIN production is seen in the very earliest stages of primordium formation [16], and intrinsic auxin production in those tissues is low [41], some simulations were begun with initial concentrations of auxin and PIN set to zero. In this case, PINs are present only if produced in response to auxin, so parameters $k_{2,PIN} = 10$ and $k_{11} = 1$ were set to compensate. Simulations under these conditions are shown in Figure 4.3. The model behaviour is similar to that seen in Figure 4.2, though slower.

The auxin production peak in this simulation spreads out symmetrically, and dissipates before sink-driven vein formation can occur. One way for this symmetry to be broken is if one side of the auxin peak nears the sink before it can diminish. Simulations with a smaller (19 x 9) leaf confirmed this, and a zone of reduced auxin concentration formed along the entire central column of cells (Fig. 4.4). This suggests that, consistent with experimental descriptions [16], perhaps midvein development begins at a very early stage, when there are only a few cells separating auxin source and sink. Increasing the amount of auxin production (by setting prod $= 100$) speeds the leaf simulation, and also allows

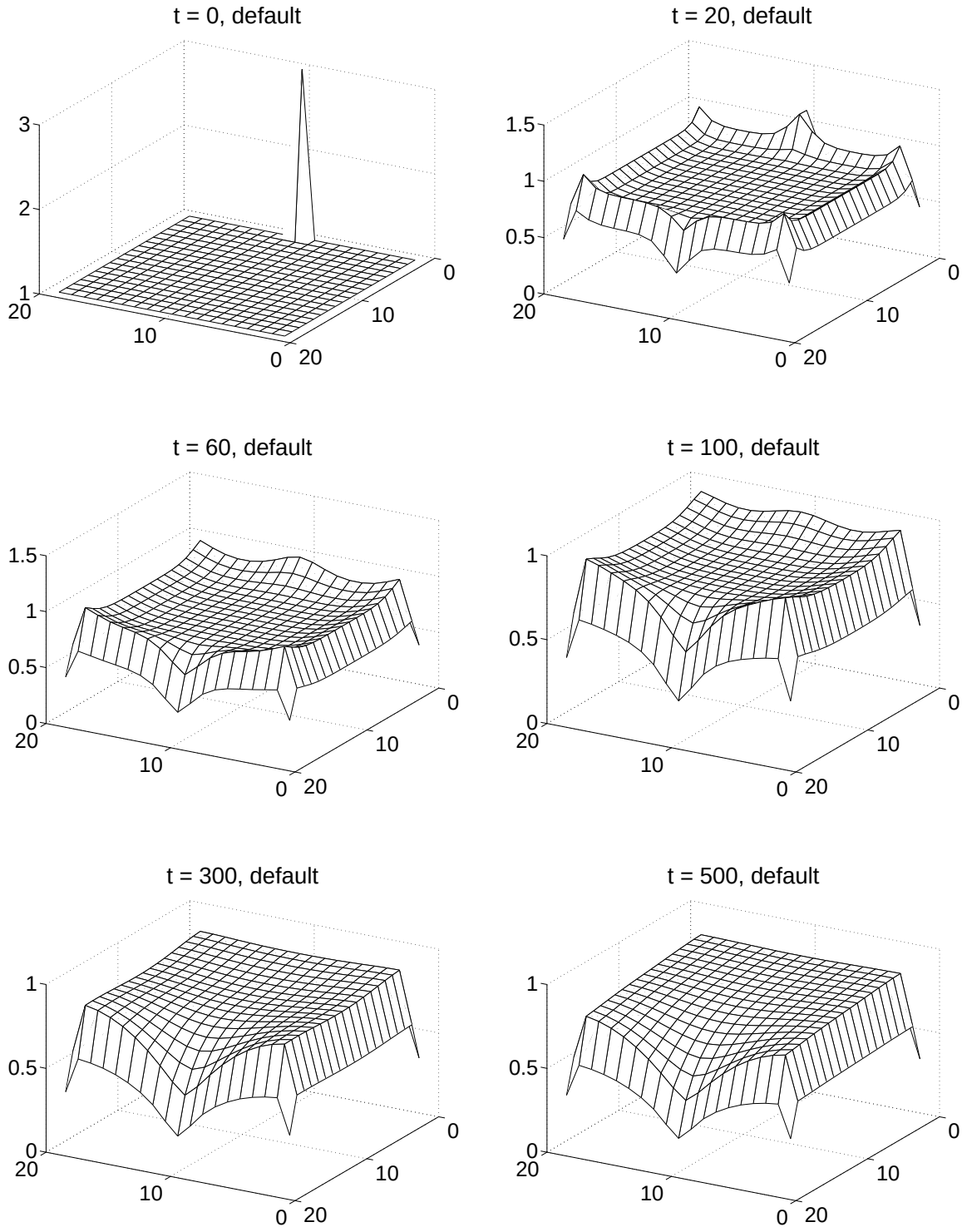

Figure 4.1: Auxin concentrations in a multicell model with parameter and initial condition defaults from single cell model, as per Tables 3.1 and 3.2. Each cell is represented by a point at the intersection of two lines, and the height of the point above the basal plane (0 on the z-axis) represents the concentration of auxin in that cell.

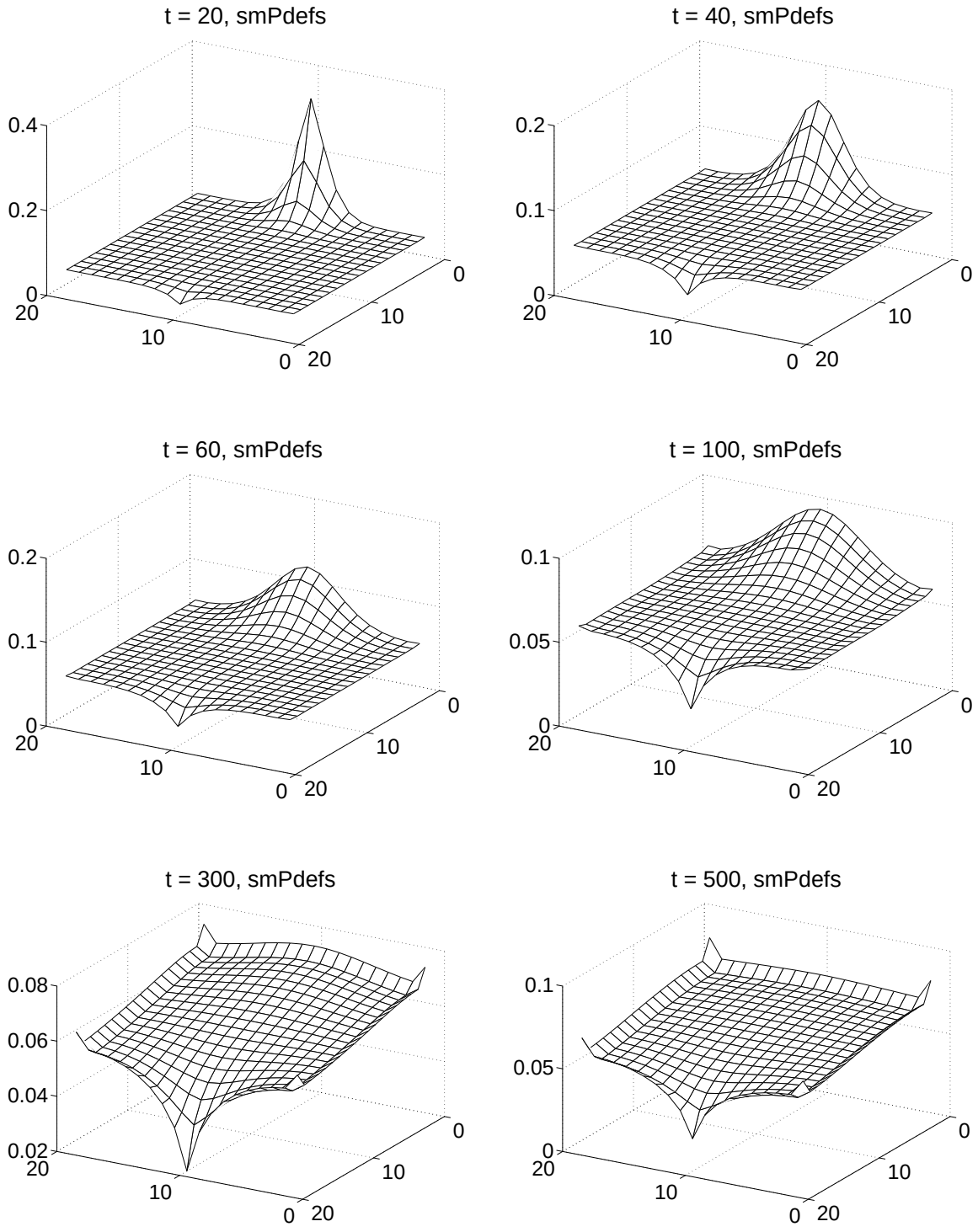

Figure 4.2: Auxin concentrations in a multicell model with parameter and initial condition defaults from single cell PIN production model. (Parameters as in Figure 4.1 except differences given in Table 3.3, and initial conditions as in Table 3.4. Axes are defined as in Figure 4.1.)

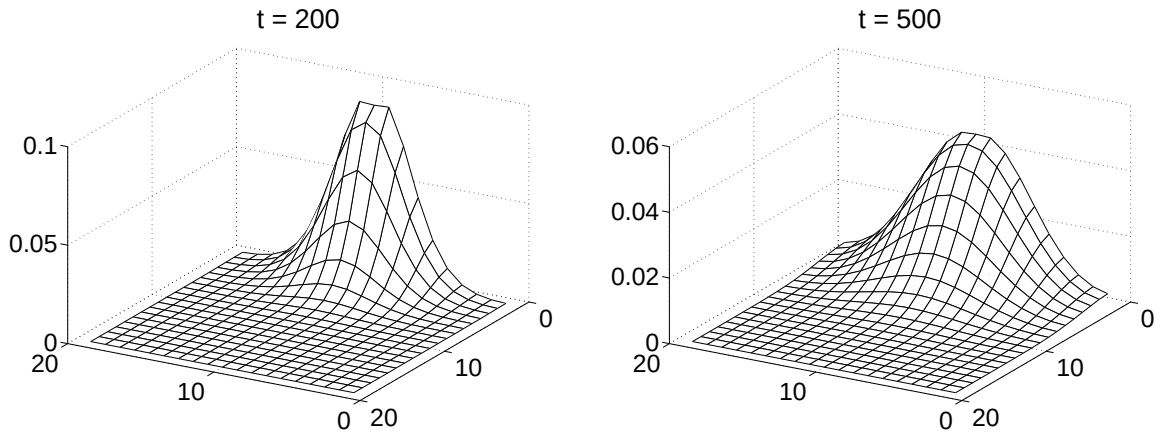

Figure 4.3: Auxin concentrations in multicell model simulation with initial conditions $[\text{auxin}_{\text{in}}] = [\text{PIN}_{\text{in}}] = [\text{PIN}_{\text{out}}]_{\text{j}} = 0$, and parameters $k_{2,PIN} = 10$ and $k_{11} = 1$. All other conditions, and axis definitions, as in Figure 4.1.

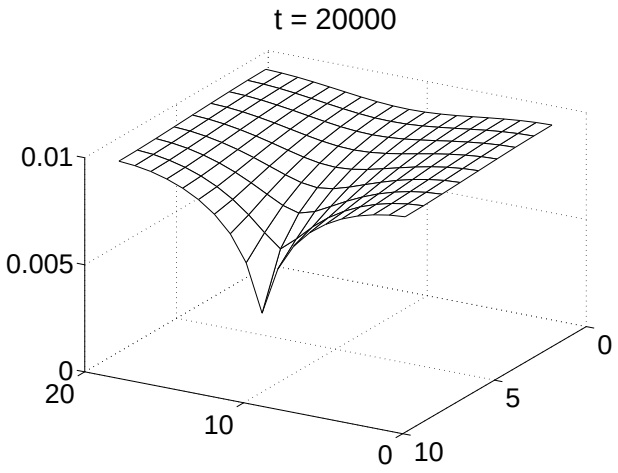

Figure 4.4: Auxin concentrations in multicell model simulation with $\text{N}_{\text{rows}} = 9$ and other conditions as in Figure 4.3. Axes are defined as in Figure 4.1.

a better view of the interesting wave-like transition from a high-auxin peak at the source to low auxin concentration along the entire central column (Figure 4.5). Note that the disappearance of the auxin peak at the leaf tip shown here is inconsistent with continued *DR5::GUS* expression seen *in vivo* over several days [16, 182].

In no simulation was there any sign of vein loops, which would not in any case be expected to form until new epidermal convergence points form [16] and the original one at the tip ceases functioning (presumably after midvein differentiation). The simulated 'vein'

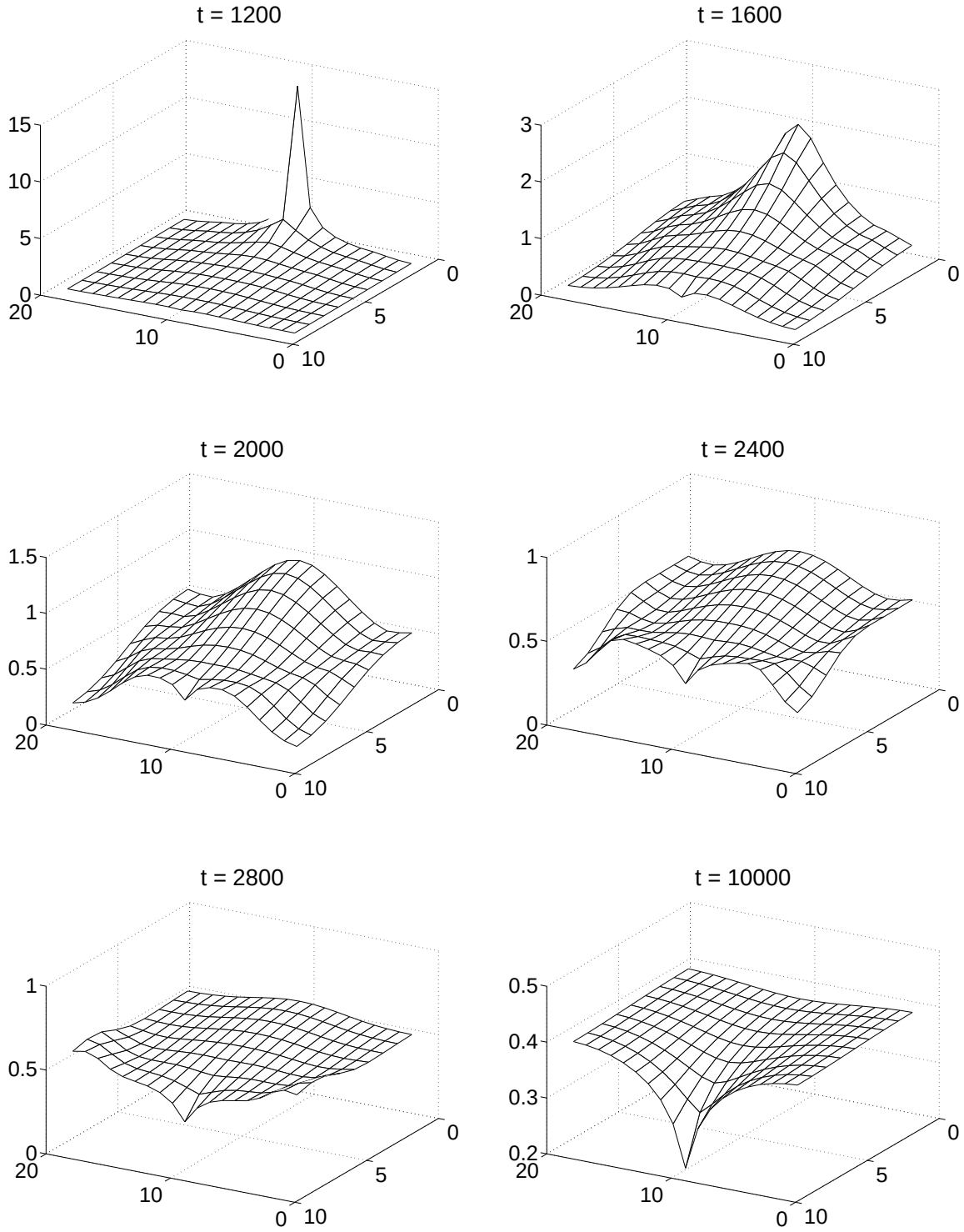

Figure 4.5: Auxin concentrations in multicell model simulation with $\mathrm{prod} = 100$ and other conditions as in Figure 4.4. Axes are defined as in Figure 4.1.

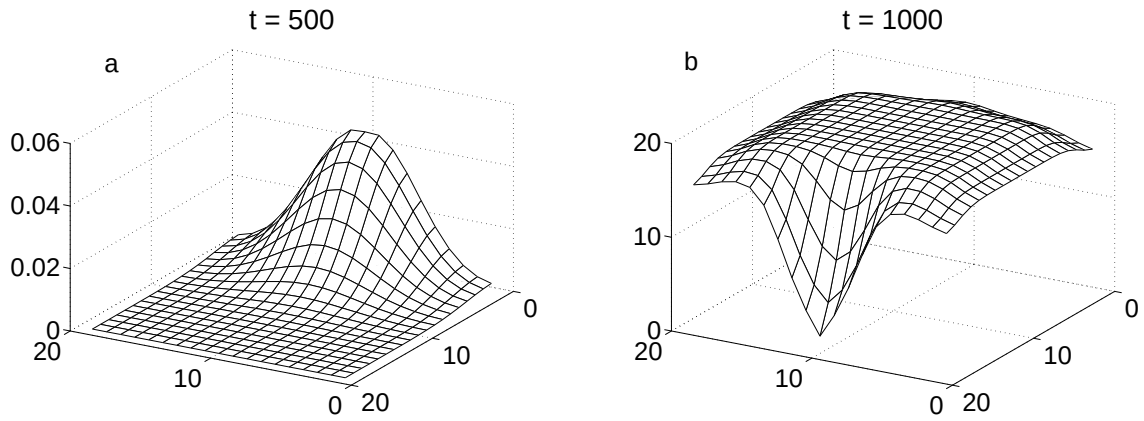

Figure 4.6: Auxin concentrations in multicell model simulations with $n \neq 1$. (a) $n = 10$, with all other conditions as in Fig. 4.3. (b) $n = -0.1$, with default conditions except $[\text{auxin}_{\text{out}}]_{\text{j}} = 10$, prod $= 10$, $k_{2,PIN} = 10$, $k_{11} = 0.1$. Axes are defined as in Figure 4.1.

analogues seen are also only fairly broad zones of depleted auxin, not the narrow files of high auxin expected on the basis of [16]. As described in Section 3.7, more pronounced PIN localization can be seen for higher values of exponent *n*. Simulations under these conditions, though, showed results similar to those performed with $n = 1$ (Fig. 4.6a). As shown in Figure 4.6b, negative values of *n* do not lead to dramatically different behaviour either; the central area still displays a low relative auxin concentration. This may be due in part to the way the petiole connection is implemented, which is an area for future consideration.

Despite the limitations of the model under the conditions examined to date, rudimentary auxin channel formation is seen to be at least possible with the multicell extension of our single-cell model. It is hoped that a more comprehensive exploration of the multicell model will reveal parameter conditions leading to more realistic results.

Chapter 5

Conclusion

5.1 Summary

The patterns of veins in plant leaves are a ubiquitous example of biological patterning, so much so that we often don't consider the complexity and variety of these patterns at all. When time is taken to look for examples, the range of forms found in different species is breathtaking. Even greater astonishment is provoked when one considers that the observed final products – complete venation networks – are not the result of previously determined schematics that plants just have to follow as they develop. Rather, the veins so vital to the plants' well-being are generated *de novo* along with each new organ, in a manner that is flexible enough to develop a connected, functional distribution system despite environmental perturbations. It is no wonder, then, that vein patterning has attracted the interest of multiple groups interested in modelling the phenomenon mathematically.

Models have been developed to provide insights into many aspects of auxin-mediated patterning. Several of these models generate visually pleasing results, but are not necessarily linked to any particular system [80, 83, 96]. Even specific vein-formation models may be relatively abstract [93]. Recent advances in genetic and biochemical studies, especially using the model plant *Arabidopsis thaliana*, have made possible models that specifically examine the role of auxin-related cellular components [79, 84, 184]. Many are predicated on the canalization hypothesis of Sachs [66, 68], which supposes that auxin flow through a cell feeds back to increase the auxin transport capacity of the cell. Under this condition, random variations in auxin distribution lead to the development of preferred strands of auxin flow, presumed to inform subsequent vein differentiation [69, 71, 74].

The transport of auxin is closely linked to its intricate and well-studied signalling pathways [62, 104, 105]. Existing models for auxin behaviour tend to focus primarily or exclusively on transporter behaviour. Enough biological data on auxin-mediated signalling

has now accrued, however, to make possible reasonable guesses at the molecular interactions underlying auxin's effects in both signalling and transport [105–108]. With these data in hand, the time was ripe for a molecular-level model to investigate the cellular basis of auxin's effects. My goal in this thesis has been to describe the development of a model incorporating both auxin signalling and transport mechanisms.

Starting from a kinetic treatment of presumed molecular interactions, a differential equation model was derived to describe the temporal dynamics of molecular species. In simulations, this simple model showed biologically plausible responses to auxin application. Interestingly, however, the modelled auxin-responsive network was unable to induce the cell to adopt a permanently polarized auxin-transporting fate. This is consistent with recent experimental results showing that the reorganization of auxin flow paths predates the expression of even the earliest known procambial gene markers [16]. Expression of auxin transporters occurs in a diffuse zone that then narrows to a single file of cells, much as envisioned in the canalization hypothesis. Canalization of flow into connected strands of auxin-transporting cells occurs even in mutant plants that are characterized by discontinuous vein formation [16, 60, 77]. This suggests that some component not included in our model, perhaps connected to procambial development genes expressed during vascular differentiation, is involved in establishing permanent polar auxin transport.

5.2 Discussion

The model presented in this thesis is highly simplified relative to biological reality. Indeed, any useful model of a complex system must be, in some sense, 'wrong' – if it included all the attributes of the original system, it would have very little utility as a model! [115] Nevertheless, there are a number of areas of the model presented that could be expanded upon if certain additional phenomena, particularly mutant phenotypes, are to be simulated fully.

The auxin signalling network included in Chapter 2 comprises a single self-regulating Aux/IAA protein, interacting with a single type of ARF. In arabidopsis, the Aux/IAAs comprise a family of 29 members, with some redundancy, but also a wide range of different behaviours and expression patterns [134, 185, 186]. For example, *IAA3/SHY2* and *IAA17/AXR3* mutant plants display opposite phenotypic effects [105]. Aux/IAAs are degraded by protein complexes which have their target specificity conferred by F-box proteins, of which there are some 700 in arabidopsis [139, 140, 187]. The regulatory complexity available in such a system supplies more than enough material for detailed investigation through a separate model, even in isolation from downstream effects. Nevertheless, at least a little more of this signalling web could be fruitfully added to this model eventually. This would, of course, necessitate a reconsideration of the simplifications introduced in Section 3.2.

Differing behaviours of various Aux/IAAs, ARFs and other proteins in distinct cell types could also explain some apparent contradictions in auxin transport behaviour. In a 2003 model of auxin-mediated phyllotactic patterning in the shoot apical meristem (SAM), for example, Reinhardt *et al.* require auxin to be preferentially transported in the direction of a local auxin maximum [65]. The model developed here is founded on exactly the opposite hypothesis: auxin is transported by PINs away from areas of auxin accumulation, and toward regions with lower concentrations. This discrepancy may be due to different regulatory circuits operating in leaves than in the SAM. That such cell-type-specific differences can occur is amply demonstrated in studies of arabidopsis roots, where even neighbouring files of cells can have completely opposite auxin transporter polarization [160].

Observed changes in transporter polarity could be due to *de novo* transcription of PINs, or merely to a redistribution of existing proteins. Experimental results have shown that transport polarity changes in roots do not depend upon transcription of new PINs [104], and that cellular PIN levels change relatively slowly [155]. Nevertheless, *PIN* genes are transcriptionally activated by auxin [16, 109, 168, 182, 188, 189], and are regulated through

the Aux/IAA—ARF pathway [104, 168]. There are also suggestions that auxin can induce PIN downregulation [109, 168] and even specific PIN degradation, possibly via a proteasomal pathway [190, 191]. Many of these responses are tissue-, cell-, time- and concentration-dependent [43, 104, 168, 176], leaving a substantial lack of clarity on the relevance of auxin-mediated *PIN* transcription. Therefore, model variants with either PIN upregulation by auxin or a constant total level of PIN were considered (Section 3.4). Much of the behaviour of both model versions is the same, which suggests that it may be difficult to distinguish between the two situations experimentally. The most significant difference between the results of the two variants is in the internal cellular concentration of auxin. As outlined in Section 3.5, having PINs produced in response to auxin means that the level of auxin inside the cell at equilibrium is lower than that in the extracellular space. Model cells with a fixed, limited level of PINs, on the other hand, develop a high internal auxin concentration relative to the cell exterior. This is consistent with simulation results reported by Feugier *et al.*, whose quite different modelling approach also showed that auxin-responsive PIN production results in vein cells with auxin concentrations lower than external levels, while competition for a limited pool of PINs produces vein cells with auxin concentrations higher than their surroundings [84].

The idea of vein cells having high auxin concentrations is contrary to the naive expectation of veins acting as sinks in early canalization models [69, 71]. There is experimental evidence from several species, howevever, that cambial cells are enriched in auxin relative to surrounding cells [18, 41, 60, 184, 192, 193]. *PIN* transcriptional regulation by auxin seems obviously useful, providing an additional level of feedback for auxin-mediated control. According to the model results discussed above, this would imply a low internal auxin concentration. However, auxin-regulated PINs and high auxin in veins are not necessarily mutually exclusive. It would be beneficial for developmental control if plant tissues were able to accumulate auxin even against a concentration gradient, and Kramer [184] has suggested that this could be accomplished by, for example, two sets of transporters:

one to move auxin polarly in transport channels (as included in our model), and a second to accumulate auxin in the strand from bordering cells. The lack of the putative second auxin accumulation system in our model could perhaps account for the fact that auxin concentrations in the extracellular spaces of the multicell model are considerably lower than intracellular auxin levels in both production and competition models. It is also important to note that all multicell simulations performed – with either PIN production or competition scenarios – display relatively low auxin concentration in putative vein areas. This seems to be linked to the way the petiole is modelled, and merits further investigation.

The function of auxin as a differentiation signal within provascular tissues brings up an interesting question: just what is it about auxin that cells are interpreting? Many models of the auxin transport system are phrased in terms of auxin flux [69–71, 79, 84, 85], and for these models it is "implicitly assumed that there is a mechanism for measuring the auxin flux leaving a cell" [71]. The model developed here, on the other hand, is formulated with PIN polarization responding to the concentration of auxin, not the flux. The exact mechanism for auxin sensing remains unclear, but there certainly does seem to be some cellular capacity to respond to auxin concentrations. Discussions of root gravitropism are usually phrased in terms of altered auxin accumulation, and it is a high concentration of auxin that inhibits cell elongation [194]. In auxin transport mutants, extra veins form along the leaf margin, where high auxin concentrations occur but flux is reduced [17]. It has also been shown that it is active auxin, rather than functioning auxin transport, that influences PIN expression in roots [168]. On the other hand, Sachs carried out an experiment where auxin was provided in such a way that no flux was possible. Under these conditions, no vessel differentiation occurred. When an outlet was provided, however, veins began to differentiate in the direction of the resultant flux [67]. Similarly, in tobacco cells it is "auxin polar transport, and not auxin per se, [that] mediates pattern formation" [195]. The highly interconnected regulation of auxin transport, polarity and signalling causes difficulties in separating auxin flux and concentration effects of auxin transporters. Alterations in polar

auxin transport certainly affect patterning [196–198], but it is often unclear whether it is the transport *per se*, or the delivery of auxin and resulting accumulation, that is causing the observed effects [199]. It is certainly possible that different signalling pathways could respond to both concentration and flux.

So how is the auxin signal – whatever it is – measured by the cell? Since auxin transport is so central to both polarity and signalling, the transporter proteins are obvious candidates for involvement. In *Escherichia coli*, it has been shown that glucose-6-phosphate (Glc6P) transporter protein UhpC is also a sensor for external Glc6P concentration [200]. By analogy, perhaps PIN or AUX1 proteins could have roles as sensors in addition to their transport capacity. Cell measurement of efflux through efflux transporters was already suggested by Mitchison, who also made the point that this would not be sufficient if diffusion was the main method of auxin entry to the cell, because many of the ejected molecules would simply reenter the cell and upset the accounting [71]. He proposed that specific auxin uptake channels could, however inefficiently, remove the difficulty. The finding that active auxin influx is more important than diffusion in most tissues [28] suggests that counting of molecules by transporters is at least feasible. Alternatively, the non-catalytic NPA-binding component of the auxin efflux complex might play a role [40, 201], or there may be a (so far unknown) cell-surface auxin receptor [141].

The success of auxin-mediated patterning in plants is due at least in part to its great adaptibility. It would be undesirable to have cell identity determined too early in development; in order to respond to developmental and environmental cues, the growing leaf must maintain its plasticity until a stable pattern is formed, which can then be made permanent by further differentiation. Such fixed cell fate – and the permanent polarization it implies – is not seen in the undifferentiated cells modelled here, even when subjected to large inputs of auxin under varying circumstances. These results are consistent with experimental findings by Scarpella and others [15, 16], who have shown that the earliest anatomically visible vein precursors actually occur rather late in auxin response, and are preceded by stages

which are much more plastic. It is at these earlier stages that auxin-conductive pathways are set up, which (in wild-type plants at least) subsequently inform the locations of vascular differentiation. This 'staged' concept of auxin-responsive vein formation also helps to explain experimental results seemingly contradictory to the idea of canalization, such as the vascular islands reported by Koizumi *et al.* [77] In such cases, the initial completely connected pattern of auxin-conducting cells suffers fragmentation due to faults in further development. Canalization in its purest form seems to occur at the very early stage of leaf development investigated in this thesis, and multicell simulations suggest that it first establishes strands of high auxin transport while the primordium is still very small.

Both Feugier *et al.*'s model mentioned above [84] and that of Dimitrov and Zucker, which deals only with auxin diffusion [94], assume auxin to be produced everywhere in the leaf. Much remains unknown about auxin production and degradation [202]. A certain low level of leaf-wide auxin production seems likely, though perhaps not at the earliest stages of development [41]. Others have argued for more localized auxin production zones [55, 203], though Scarpella *et al.*'s recent results mentioned above suggest that these specific auxin-producing areas may have been examined during leaf growth stages later than those of interest for our model. They could perhaps be a consequence rather than a cause of early patterning, and result from a quite different mechanism [16].

5.3 Prospects

"Auxin does everything" [24]. As is clear from the previous section, much remains unknown, but new insights are constantly being gained into the elegant mechanisms by which a single simple chemical can regulate such a diversity of phenomena. Auxin's unprecedented mode of TIR1 binding [204], recently revealed by X-ray crystallography [142], hints that it almost certainly has more surprises in store. As experimentalists reveal more and more of the complexity of plant biology, theoretical models will develop in parallel

and deepen our understanding still further. Hopefully the model of auxin signalling and transport developed here will have a part to play in the story.

References

[1] Murray JD (2003) *Mathematical Biology. II: Spatial Models and Biomedical Applications*. Springer, New York.

[2] Roth-Nebelsick A, Uhl D, Mosbrugger V & Kerp H (2001) Evolution and function of leaf venation architecture: A review. *Ann Bot* **87**, 553–566.

[3] Ye ZH (2002) Vascular tissue differentiation and pattern formation in plants. *Annu Rev Plant Biol* **53**, 183–202.

[4] Turner S & Sieburth LE (2003) Vascular patterning. In Somerville & Meyerowitz [205]. DOI: 10.1199/tab.0073.

[5] Kang J & Dengler N (2004) Vein pattern development in adult leaves of *Arabidopsis thaliana*. *Int J Plant Sci* **165**, 231–242.

[6] Fujita H & Mochizuki A (2006) The origin of the diversity of leaf venation pattern. *Dev Dynam* **235**, 2710–2721.

[7] Leyser O (1997) Auxin: Lessons from a mutant weed. *Physiol Plant* **100**, 407–414.

[8] Pigliucci M (2002) Ecology and evolutionary biology of *Arabidopsis*. In Somerville & Meyerowitz [205]. DOI: 10.1199/tab.0003.

[9] Al-Shehbaz IA & O'Kane SL Jr (2002) Taxonomy and phylogeny of Arabidopsis (Brassicaceae). In Somerville & Meyerowitz [205]. DOI: 10.1199/tab.0001.

[10] Rédei GP (1975) *Arabidopsis* as a genetic tool. *Annu Rev Genet* **9**, 111–127.

[11] Somerville CR & Meyerowitz EM (1994) Introduction. In Meyerowitz & Somerville [206], pp. 1–6.

[12] Telfer A & Poethig RS (1994) Leaf development in *Arabidopsis*. In Meyerowitz & Somerville [206], chap. 15, pp. 379–401.

[13] Nelson T & Dengler N (1997) Leaf vascular pattern formation. *Plant Cell* **9**, 1121–1135.

[14] Sieburth LE (1999) Auxin is required for leaf vein pattern in Arabidopsis. *Plant Physiol* **121**, 1179–1190.

[15] Scarpella E, Francis P & Berleth T (2004) Stage-specific markers define early steps of procambium development in *Arabidopsis* leaves and correlate termination of vein formation with mesophyll differentiation. *Development* **131**, 3445–3455.

[16] Scarpella E, Marcos D, Friml J & Berleth T (2006) Control of leaf vascular patterning by polar auxin transport. *Genes Dev* **20**, 1015–1027.

[17] Mattsson J, Sung ZR & Berleth T (1999) Responses of plant vascular systems to auxin transport inhibition. *Development* **126**, 2979–2991.

[18] Mattsson J, Ckurshumova W & Berleth T (2003) Auxin signaling in Arabidopsis leaf vascular development. *Plant Physiol* **131**, 1327–1339.

[19] Woodward AW & Bartel B (2005) Auxin: Regulation, action and interaction. *Ann Bot* **95**, 707–735.

[20] Normanly J, Slovin JP & Cohen JD (1995) Rethinking auxin biosynthesis and metabolism. *Plant Physiol* **107**, 323–329.

[21] Kende H & Zeevaart JAD (1997) The five "classical" plant hormones. *Plant Cell* **9**, 1197–1210.

[22] Ferro N, Bultinck P, Gallegos A, Jacobsen HJ, Carbo-Dorca R & Reinard T (2007) Unrevealed structural requirements for auxin-like molecules by theoretical and experimental evidences. *Phytochemistry* **68**, 237–250.

[23] Davies PJ (1995) The plant hormones: Their nature, occurrence, and functions. In *Plant Hormones: Physiology, Biochemistry and Molecular Biology* [207], pp. 1–12.

[24] Leyser O (2001) Auxin. *Curr Biol* **11**, R728.

[25] Perrot-Rechenmann C & Napier RM (2005) Auxins. In *Vitamins and Hormones*, vol. 72, pp. 203–233. Elsevier.

[26] Goldsmith MHM (1977) The polar transport of auxin. *Ann Rev Plant Physiol* **28**, 439–478.

[27] Lomax TL, Muday GK & Rubery PH (1995) Auxin transport. In Davies [207], pp. 509–530.

[28] Kramer EM & Bennett MJ (2006) Auxin transport: A field in flux. *Trends Plant Sci* **11**, 382–386.

[29] Rubery PH & Sheldrake AR (1974) Carrier-mediated auxin transport. *Planta (Berl)* **118**, 101–121.

[30] Raven JA (1975) Transport of indoleacetic acid in plant cells in relation to pH and electrical potential gradients, and its significance for polar IAA transport. *New Phytol* **74**, 163–172.

[31] Mitchell P (1961) Coupling of phosphorylation to electron and hydrogen transfer by a chemi-osmotic type of mechanism. *Nature* **191**, 144–148.

[32] Friml J & Palme K (2002) Polar auxin transport - old questions and new concepts? *Plant Mol Biol* **49**, 273–284.

[33] Baluška F, Šamaj J & Menzel D (2003) Polar transport of auxin: Carrier-mediated flux across the plasma membrane or neurotransmitter-like secretion? *Trends Cell Biol* **13**, 282–285.

[34] Baluška F, Mancuso S, Volkmann D & Barlow P (2004) Root apices as plant command centres: The unique 'brain-like' status of the root apex transition zone. *Biologia (Bratislava)* **39** (Suppl. 13), 1–13.

[35] Baluška F, Volkmann D & Menzel D (2005) Plant synapses: Actin-based domains for cell-to-cell communication. *Trends Plant Sci* **10**, 106–111.

[36] Stokes T (2005) Plant neurobiology sprouts anew. *The Scientist* **19**, 24.

[37] Brenner ED, Stahlberg R, Mancuso S, Vivanco J, Baluška F & Volkenburgh EV (2006) Plant neurobiology: An integrated view of plant signalling. *Trends Plant Sci* **11**, 413–419.

[38] Schlicht M, Strnad M, Scanlon MJ, Mancuso S, Hochholdinger F, Palme K, Volkmann D, Menzel D & Baluska F (2006) Auxin immunolocalization implicates vesicular neurotransmitter-like mode of polar auxin transport in root apices. *Plant Signal Beh* **1**, 122–133.

[39] Estelle M (1998) Polar auxin transport: New support for an old model. *Plant Cell* **10**, 1775–1778.

[40] Morris DA, Friml J & Zažímalová E (2004) The transport of auxins. In Davies [208], pp. 437–470.

[41] Avsian-Kretchmer O, Cheng JC, Chen L, Moctezuma E & Sung ZR (2002) Indole acetic acid distribution coincides with vascular differentiation pattern during Arabidopsis leaf ontogeny. *Plant Physiol* **130**, 199–209.

[42] Dengler N & Kang J (2001) Vascular patterning and leaf shape. *Curr Op Plant Biol* **4**, 50–56.

[43] Heisler MG, Ohno C, Das P, Sieber P, Reddy GV, Long JA & Meyerowitz EM (2005) Patterns of auxin transport and gene expression during primordium development revealed by live imaging of the *Arabidopsis* inflorescence meristem. *Curr Biol* **15**, 1899–1911.

[44] Kepinski S (2006) Integrating hormone signaling and patterning mechanisms in plant development. *Curr Op Plant Biol* **9**, 28–34.

[45] Dengler NG (2001) Regulation of vascular development. *J Plant Growth Reg* **20**, 1–13.

[46] Hay A, Barkoulas M & Tsiantis M (2004) PINning down the connections: Transcription factors and hormones in leaf morphogenesis. *Curr Op Plant Biol* **7**, 575–581.

[47] Carlsbecker A & Helariutta Y (2005) Phloem and xylem specification: Pieces of the puzzle emerge. *Curr Op Plant Biol* **8**, 512–517.

[48] Prigge MJ, Otsuga D, Alonso JM, Ecker JR, Drews GN & Clark SE (2005) Class III homeodomain-leucine zipper gene family members have overlapping, antagonistic, and distinct roles in Arabidopsis development. *Plant Cell* **17**, 61–76.

[49] Byrne ME (2006) Shoot meristem function and leaf polarity: The role of class III HD-ZIP genes. *PLoS Genet* **2**, e89 (0785–0790).

[50] Sieburth LE & Deyholos MK (2006) Vascular development: The long and winding road. *Curr Op Plant Biol* **9**, 48–54.

[51] Holding DR & Springer PS (2002) The vascular prepattern enhancer trap marks early vascular development in Arabidopsis. *Genesis* **33**, 155–159.

[52] Baima S, Possenti M, Matteucci A, Wisman E, Altamura MM, Ruberti I & Morelli G (2001) The Arabidopsis ATHB-8 HD-Zip protein acts as a differentiation-promoting transcription factor of the vascular meristems. *Plant Physiol* **126**, 643–655.

[53] Kang J & Dengler N (2002) Cell cycling frequency and expression of the homeobox gene *ATHB-8* during leaf vein development in *Arabidopsis*. *Planta* **216**, 212–219.

[54] Kang J, Tang J, Donnelly P & Dengler N (2003) Primary vascular pattern and expression of *ATHB-8* in shoots of *Arabidopsis*. *New Phytol* **158**, 443–454.

[55] Aloni R (2004) The induction of vascular tissues by auxin. In Davies [208], pp. 471–492.

[56] Ulmasov T, Hagen G & Guilfoyle TJ (1997) Aux/IAA proteins repress expression of reporter genes containing natural and highly active synthetic auxin response elements. *Plant Cell* **9**, 1963–1971.

[57] Guilfoyle TJ (1998) Aux/IAA proteins and auxin signal transduction. *Trends Plant Sci* **3**, 205–207.

[58] Bennett MJ, Marchant A, May ST & Swarup R (1998) Going the distance with auxin: Unravelling the molecular basis of auxin transport. *Phil Trans R Soc Lond B* **353**, 1511–1515.

[59] Palme K & Gälweiler L (1999) PIN-pointing the molecular basis of auxin transport. *Curr Op Plant Biol* **2**, 375–381.

[60] Koizumi K, Naramoto S, Sawa S, Yahara N, Ueda T, Nakano A, Sugiyama M & Fukuda H (2005) VAN3 ARF-GAP-mediated vesicle transport is involved in leaf vascular network formation. *Development* **132**, 1699–1711.

[61] Leyser O (2005) The fall and rise of apical dominance. *Curr Op Gen Dev* **15**, 468–471.

[62] Paciorek T, Zažímalová E, Ruthardt N, Petrášek J, Stierhof YD, Kleine-Vehn J, Morris DA, Emans N, Jürgens G, Geldner N & Friml J (2005) Auxin inhibits endocytosis and promotes its own efflux from cells. *Nature* **435**, 1251–1256.

[63] Wiśniewska J, Xu J, Seifertová D, Brewer PB, Růžička K, Blilou I, Roquie D, Benková E, Scheres B & Friml J (2006) Polar PIN localization is sufficient to direct auxin flow in plants. *Science* **312**, 883.

[64] Benková E, Michniewicz M, Sauer M, Teichmann T, Seifertová D, Jürgens G & Friml J (2003) Local, efflux-dependent auxin gradients as a common module for plant organ formation. *Cell* **115**, 591–602.

[65] Reinhardt D, Pesce ER, Stieger P, Mandel T, Baltensperger K, Bennett M, Traas J, Friml J & Kuhlemeier C (2003) Regulation of phyllotaxis by polar auxin transport. *Nature* **426**, 255–260.

[66] Sachs T (1969) Polarity and the induction of organized vascular tissues. *Ann Bot* **33**, 263–275.

[67] Sachs T (1981) The control of the patterned differentiation of vascular tissues. *Adv Bot Res* **9**, 152–262.

[68] Sachs T (2003) Collective specification of cellular development. *BioEssays* **25**, 897–903.

[69] Mitchison G (1980) A model for vein formation in higher plants. *Proc R Soc Lond B* **207**, 79–109.

[70] Mitchison G (1980) The dynamics of auxin transport. *Proc R Soc Lond B* **209**, 489–511.

[71] Mitchison G (1981) The polar transport of auxin and vein patterns in plants. *Phil Trans R Soc Lond B* **295**, 461–471.

[72] Mitchison G (1981) The effect of intracellular geometry on auxin transport. I. Centrifugation experiments. *Proc R Soc Lond B* **295**, 53–67.

[73] Mitchison G (1981) The effect of intracellular geometry on auxin transport. II. Geotropism in shoots. *Proc R Soc Lond B* **295**, 69–83.

[74] Rolland-Lagan AG & Prusinkiewicz P (2005) Reviewing models of auxin canalization in the context of leaf vein pattern formation in Arabidopsis. *Plant J* **44**, 854–865.

[75] Berleth T (2000) Plant development: Hidden networks. *Curr Biol* **10**, R658–R661.

[76] Deyholos MK, Cordner G, Beebe D & Sieburth LE (2000) The *SCARFACE* gene is required for cotyledon and leaf vein patterning. *Development* **127**, 3205–3213.

[77] Koizumi K, Sugiyama M & Fukuda H (2000) A series of novel mutants of *Arabidopsis thaliana* that are defective in the formation of continuous vascular network: Calling the auxin signal flow canalization hypothesis into question. *Development* **127**, 3197–3204.

[78] Sieburth LE, Muday GK, King EJ, Benton G, Kim S, Metcalf KE, Meyers L, Seamen E & Norman JMV (2006) *SCARFACE* encodes an ARF-GAP that is required for normal auxin efflux and vein patterning in *Arabidopsis*. *Plant Cell* **18**, 1396–1411.

[79] Feugier FG & Iwasa Y (2006) How canalization can make loops: A new model of reticulated leaf vascular pattern formation. *J Theor Biol* **243**, 235–244.

[80] Meinhardt H (1976) Morphogenesis of lines and nets. *Differentiation* **6**, 117–123.

[81] Koch AJ & Meinhardt H (1994) Biological pattern formation: From basic mechanisms to complex structures. *Rev Mod Phys* **66**, 1481–1507.

[82] Meinhardt H (1995) Development of higher organisms: How to avoid error propagation and chaos. *Physica D* **86**, 96–103.

[83] Meinhardt H (1996) Models of biological pattern formation: Common mechanism in plant and animal development. *Int J Dev Biol* **40**, 123–134.

[84] Feugier FG, Mochizuki A & Iwasa Y (2005) Self-organization of the vascular system in plant leaves: Inter-dependent dynamics of auxin flux and carrier proteins. *J Theor Biol* **236**, 366–375.

[85] Fujita H & Mochizuki A (2006) Pattern formation of leaf veins by the positive feedback regulation between auxin flow and auxin efflux carrier. *J Theor Biol* **241**, 541–551.

[86] Steynen QJ & Schultz EA (2003) The FORKED genes are essential for distal vein meeting in *Arabidopsis*. *Development* **130**, 4695–4708.

[87] Carland FM & Nelson T (2004) *COTYLEDON VASCULAR PATTERN2*-mediated inositol (1,4,5) triphosphate signal transduction is essential for closed venation patterns of Arabidopsis foliar organs. *Plant Cell* **16**, 1263–1275.

[88] Leopold AC & Hall OF (1966) Mathematical model of polar auxin transport. *Plant Physiol* **41**, 1476–1480.

[89] Goldsmith MHM, Goldsmith TH & Martin MH (1981) Mathematical analysis of the chemiosmotic polar diffusion of auxin through plant tissues. *Proc Natl Acad Sci USA* **78**, 976–980.

[90] Martin MH, Goldsmith MHM & Goldsmith TH (1990) On polar auxin transport in plant cells. *J Math Biol* **28**, 197–223.

[91] Kramer EM (2002) A mathematical model of pattern formation in the vascular cambium of trees. *J Theor Biol* **216**, 147–158.

[92] Forest L, Padilla F, Martínez S, Demongeot J & Martín JS (2006) Modelling of auxin transport affected by gravity and differential radial growth. *J Theor Biol* **241**, 241–251.

[93] Runions A, Fuhrer M, Lane B, Federl P, Rolland-Lagan AG & Prusinkiewicz P (2005) Modeling and visualization of leaf venation patterns. *ACM Trans Graphics* **24**, 702–711.

[94] Dimitrov P & Zucker SW (2006) A constant production hypothesis guides leaf venation patterning. *Proc Natl Acad Sci USA* **103**, 9363–9368.

[95] Markus M, Böhm D & Schmick M (1999) Simulation of vessel morphogenesis using cellular automata. *Math Biosci* **156**, 191–206.

[96] Couder Y, Pauchard L, Allain C, Adda-Bedia M & Douady S (2002) The leaf venation as formed in a tensorial field. *Eur Phys J B* **28**, 135–138.

[97] Dumais J (2007) Can mechanics control pattern formation in plants? *Curr Op Plant Biol* **10**, 58–62.

[98] de Reuille PB, Bohn-Courseau I, Ljung K, Morin H, Carraro N, Godin C & Traas J (2006) Computer simulations reveal properties of the cell-cell signaling network at the shoot apex in *Arabidopsis*. *Proc Natl Acad Sci USA* **103**, 1627–1632.

[99] Heisler MG & Jönsson H (2006) Modelling auxin transport and plant development. *J Plant Growth Reg* **25**, 302–312.

[100] Jönsson H, Heisler MG, Shapiro BE, Meyerowitz EM & Mjolsness E (2006) An auxin-driven polarized transport model for phyllotaxis. *Proc Natl Acad Sci USA* **103**, 1633–1638.

[101] Smith RS, Guyomarc'h S, Mandel T, Reinhardt D, Kuhlemeier C & Prusinkiewicz P (2006) A plausible model of phyllotaxis. *Proc Nat Acad Sci USA* **103**, 1301–1306.

[102] Hellwig H, Engelmann R & Deussen O (2006) Contact pressure models for spiral phyllotaxis and their computer simulation. *J Theor Biol* **240**, 489–500.

[103] Heisler MG & Jönsson H (2007) Modelling meristem development in plants. *Curr Op Plant Biol* **10**, 92–97.

[104] Sauer M, Balla J, Luschnig C, Wisniewska J, Reinöhl V, Friml J & Benková E (2006) Canalization of auxin flow by Aux/IAA-ARF-dependent feedback regulation of PIN polarity. *Genes Dev* **20**, 2902–2911.

[105] Leyser O (2006) Dynamic integration of auxin transport and signalling. *Curr Biol* **16**, R424–R433.

[106] Callis J (2005) Auxin action. *Nature* **435**, 436–437.

[107] Hobbie L (2005) Seek and ye shall [eventually] find: The end of the search for the auxin receptor. *J Integ Plant Biol* **47**, 1412–1417.

[108] Berleth T, Scarpella E & Prusinkiewicz P (2007) Towards the systems biology of auxin-transport-mediated patterning. *Trends Plant Sci* **12**, 151–159.

[109] Vieten A, Sauer M, Brewer PB & Friml J (2007) Molecular and cellular aspects of auxin-transport-mediated development. *Trends Plant Sci* **12**, 160–168.

[110] Kerr ID & Bennett MJ (2007) New insight into the biochemical mechanisms regulating auxin transport in plants. *Biochem J* **401**, 613–622.

[111] Quint M & Gray WM (2006) Auxin signaling. *Curr Op Plant Biol* **9**, 448–453.

[112] Paciorek T & Friml J (2006) Auxin signaling. *J Cell Sci* **119**, 1199–1202.

[113] Endy D & Brent R (2001) Modelling cellular behaviour. *Nature* **409**, 391–395.

[114] Prusinkiewicz P (2004) Modeling plant growth and development. *Curr Op Plant Biol* **7**, 79–83.

[115] Kollmann M & Sourjik V (2007) *In Silico* biology: From simulation to understanding. *Curr Biol* **17**, R132–R134.

[116] Libbenga KR & Mennes AM (1995) Hormone binding and signal transduction. In Davies [207], pp. 272–297.

[117] Timpte C (2001) Auxin binding protein: Curiouser and curiouser. *Trends Plant Sci* **6**, 586–590.

[118] Napier RM, David KM & Perrot-Rechenmann C (2002) A short history of auxin-binding proteins. *Plant Mol Biol* **49**, 339–348.

[119] Jones AM & Prasad PV (1992) Auxin-binding proteins and their possible roles in auxin-mediated plant cell growth. *BioEssays* **14**, 43–48.

[120] Leblanc N, Perrot-Rechenmann C & Barbier-Brygoo H (1999) The auxin-binding protein Nt-ERabp1 alone activates an auxin-like transduction pathway. *FEBS Lett* **449**, 57–60.

[121] Woo EJ, Marshall J, Bauly J, Chen JG, Venis M, Napier RM & Pickersgill RW (2002) Crystal structure of auxin-binding protein 1 in complex with auxin. *EMBO J* **21**, 2877–2885.

[122] Woodward AW & Bartel B (2005) A receptor for auxin. *Plant Cell* **17**, 2425–2429.

[123] Abel S & Theologis A (1996) Early genes and auxin action. *Plant Physiol* **111**, 9–17.

[124] Ulmasov T, Hagen G & Guilfoyle TJ (1997) ARF1, a transcription factor that binds auxin response elements. *Science* **276**, 1865–1868.

[125] Ulmasov T, Hagen G & Guilfoyle TJ (1999) Dimerization and DNA binding of auxin response factors. *Plant J* **19**, 309–319.

[126] Guilfoyle T, Hagen G, Ulmasov T & Murfett J (1998) How does auxin turn on genes? *Plant Physiol* **118**, 341–347.

[127] Guilfoyle TJ, Ulmasov T & Hagen G (1998) The ARF family of transcription factors and their role in plant hormone-responsive transcription. *Cell Mol Life Sci* **54**, 619–627.

[128] Guilfoyle TJ & Hagen G (2001) Auxin response factors. *J Plant Growth Reg* **20**, 281–291.

[129] Tiwari SB, Hagen G & Guilfoyle T (2003) The roles of auxin response factor domains in auxin-responsive transcription. *Plant Cell* **15**, 533–543.

[130] Dharmasiri N & Estelle M (2004) Auxin signaling and regulated protein degradation. *Trends Plant Sci* **9**, 1360–1385.

[131] Abel S, Oeller PW & Theologis A (1994) Early auxin-induced genes encode short-lived nuclear proteins. *Proc Natl Acad Sci USA* **91**, 326–330.

[132] Tiwari SB, Wang XJ, Hagen G & Guilfoyle T (2001) AUX/IAA genes are active repressors, and their stability and activity are modulated by auxin. *Plant Cell* **13**, 2809–2822.

[133] Kim J, Harter K & Theologis A (1997) Protein-protein interactions among the Aux/IAA proteins. *Proc Natl Acad Sci USA* **94**, 11786–11791.

[134] Dreher KA, Brown J, Saw RE & Callis J (2006) The *Arabidopsis* Aux/IAA protein family has diversified in degradation and auxin responsiveness. *Plant Cell* **18**, 699–714.

[135] Callis J & Vierstra RD (2000) Protein degradation in signaling. *Curr Op Plant Biol* **3**, 381–386.

[136] Ciechanover A (1998) The ubiquitin-proteasome pathway: On protein death and cell life. *EMBO J* **17**, 7151–7160.

[137] Ciechanover A & Schwartz AL (1998) The ubiquitin-proteasome pathway: The complexity and myriad functions of proteins death. *Proc Natl Acad Sci USA* **95**, 2727–2730.

[138] Ciechanover A, Orian A & Schwartz AL (2000) Ubiquitin-mediated proteolysis: Biological regulation via destruction. *BioEssays* **22**, 442–451.

[139] Dharmasiri N, Dharmasiri S & Estelle M (2005) The F-box protein TIR1 is an auxin receptor. *Nature* **435**, 441–445.

[140] Kepinski S & Leyser O (2005) The *Arabidopsis* F-box protein TIR1 is an auxin receptor. *Nature* **435**, 446–451.

[141] Badescu GO & Napier RM (2006) Receptors for auxin: Will it all end in TIRs? *Trends Plant Sci* **11**, 217–223.

[142] Tan X, Calderon-Villalobos LIA, Sharon M, Zheng C, Robinson CV, Estelle M & Zheng N (2007) Mechanism of auxin perception by the TIR1 ubiquitin ligase. *Nature* **446**, 640–645.

[143] Bennett MJ, Marchant A, Green HG, May ST, Ward SP, Millner PA, Walker AR, Schulz B & Feldmann KA (1996) *Arabidopsis AUX1* gene: a permease-like regulator of root gravitropism. *Science* **273**, 948–950.

[144] Yang Y, Hammes UZ, Taylor CG, Schachtman DP & Nielsen E (2006) High-affinity auxin transport by the AUX1 influx carrier protein. *Curr Biol* **16**, 1–5.

[145] Benjamins R, Malenica N & Luschnig C (2005) Regulating the regulator: The control of auxin transport. *BioEssays* **27**, 1246–1255.

[146] Hobbie LJ (2006) Auxin and cell polarity: The emergence of AXR4. *Trends Plant Sci* **11**, 517–518.

[147] Dharmasiri S, Swarup R, Mockaitis K, Dharmasiri N, Singh SK, Kowalchyk M, Marchant A, Mills S, Sandberg G, Bennett MJ & Estelle M (2006) AXR4 is required for localization of the auxin influx facilitator AUX1. *Science* **312**, 1218–1220.

[148] Chen R, Hilson P, Sedbrook J, Rosen E, Caspar T & Masso PH (1998) The *Arabidopsis thaliana AGRAVITROPIC 1* gene encodes a component of the polar-auxin-transport efflux carrier. *Proc Natl Acad Sci USA* **95**, 15112–15117.

[149] Morris DA (2000) Transmembrane auxin carrier systems - dynamic regulators of polar auxin transport. *Plant Growth Reg* **32**, 161–172.

[150] Blakeslee JJ, Peer WA & Murphy AS (2005) Auxin transport. *Curr Op Plant Biol* **8**, 1–7.

[151] Petrášek J, Mravec J, Bouchard R, Blakeslee JJ, Abas M, Seifertová D, Wiśniewska J, Tadele Z, Kubeš M, Čovanová M, Dhonukshe P, Skůpa P *et al.* (2006) PIN proteins perform a rate-limiting function in cellular auxin efflux. *Science* **312**, 914–918.

[152] Geisler M, Blakeslee JJ, Bouchard R, Lee OR, Vincenzetti V, Bandyopadhyay A, Titapiwatanakun B, Peer WA, Bailly A, Richards EL, Ejendal KFK, Smith AP *et al.* (2005) Cellular efflux of auxin catalyzed by the Arabidopsis MDR/PGP transporter AtPGP1. *Plant J* **44**, 179–194.

[153] Blakeslee JJ, Peer WA & Murphy AS (2005) MDR/PGP auxin transport proteins and endocytic cycling. In *Plant Endocytosis* (Šamaj J, Baluška F & Menzel D, eds.), Plant Cell Monographs(1), pp. 159–176. Springer, Berlin / Heidelberg.

[154] Steinmann T, Geldner N, Grebe M, Mangold S, Jackson CL, Paris S, Gälweiler L, Palme K & Jürgens G (1999) Coordinated polar localization of auxin efflux carrier PIN1 by GNOM ARF GEF. *Science* **286**, 316–318.

[155] Geldner N, Friml J, Stierhof YD, Jürgens G & Palme K (2001) Auxin transport inhibitors block PIN1 cycling and vesicle trafficking. *Nature* **413**, 425–428.

[156] Geldner N, Anders N, Wolters H, Keicher J, Kornberger W, Muller P, Delbarre A, Ueda T, Nakano A & Jürgens G (2003) The *Arabidopsis* GNOM ARF-GEF mediates endosomal recycling, auxin transport, and auxin-dependent plant growth. *Cell* **112**, 141–142.

[157] Geldner N, Richter S, Vieten A, Marquardt S, Torres-Ruiz RA, Mayer U & Jürgens G (2003) Partial loss-of-function alleles reveal a role for *GNOM* in auxin transport-related, post-embryonic development of *Arabidopsis*. *Development* **131**, 389–400.

[158] Petrášek J, Černá A, Schwarzerová K, Elčkner M, Morris DA & Zažímalová E (2003) Do phytotropins inhibit auxin efflux by impairing vesicle traffic? *Plant Physiol* **131**, 254–263.

[159] Swarup R, Friml J, Marchant A, Ljung K, Sandberg G, Palme K & Bennett M (2001) Localization of the auxin permease AUX1 suggests two functionally distinct hormone transport pathways operate in the *Arabidopsis* root apex. *Genes Dev* **15**, 2648–2653.

[160] Kleine-Vehn J, Dhonukshe P, Swarup R, Bennett M & Friml J (2006) Subcellular trafficking of the *Arabidopsis* auxin influx carrier AUX1 uses a novel pathway distinct from PIN1. *Plant Cell* **18**, 3171–3181.

[161] Cande WZ & Ray PM (1976) Nature of cell-to-cell transfer of auxin in polar transport. *Planta (Berl)* **129**, 43–52.

[162] Ermentrout B (2002) *Simulating, Analyzing and Animating Dynamical Systems: A Guide to XPPAUT for Researchers and Students*. Society for Industrial and Applied Mathematics, Philadelphia, PA.

[163] Napier RM (2005) TIRs of joy: New receptors for auxin. *BioEssays* **27**, 1213–1217.

[164] Reed JW (2001) Roles and activities of Aux/IAA proteins in *Arabidopsis*. *Trends Plant Sci* **6**, 420–425.

[165] Weijers D, Benkova E, Jäger KE, Schlereth A, Hamann T, Kientz M, Wilmoth JC, Reed JW & Jürgens G (2005) Developmental specificity of auxin response by pairs of ARF and Aux/IAA transcriptional regulators. *EMBO J* **24**, 1874–1885.

[166] Ouellet F, Overvoorde PJ & Theologis A (2001) IAA17/AXR3: Biochemical insight into an auxin mutant phenotype. *Plant Cell* **13**, 829–841.

[167] Abel S, Ballas N, Wong LM & Theologis A (1996) DNA elements responsive to auxin. *BioEssays* **18**, 647–654.

[168] Vieten A, Vanneste S, Wiśniewska J, Benková E, Benjamins R, Beeckman T, Luschnig C & Friml J (2005) Functional redundancy of PIN proteins is accompanied by auxin-dependent cross-regulation of PIN expression. *Development* **132**, 4521–4531.

[169] Abel S, Nguyen D & Theologis A (1995) The *PS-IAA4/5*-like family of early auxin-inducible mRNAs in *Arabidopsis thaliana*. *J Mol Biol* **251**, 533–549.

[170] Dhonukshe P, Kleine-Vehn J & Friml J (2005) Cell polarity, auxin transport, and cytoskeleton-mediated division planes: Who comes first? *Protoplasma* **226**, 67–73.

[171] Chasan R (1994) Tracing tracheary element development. *Plant Cell* **6**, 917–919.

[172] Church DL (1993) Tracheary element differentiation in *Zinnia* mesophyll cell cultures. *Plant Growth Reg* **12**, 179–188.

[173] Demura T & Fukuda H (1994) Novel vascular cell-specific genes whose expression is regulated temporally and spatially during vascular system development. *Plant Cell* **6**, 967–981.

[174] Benjamins R, Quint A, Weijers D, Hooykaas P & Offringa R (2001) The PINOID protein kinase regulates organ development in *Arabidopsis* by enhancing polar auxin transport. *Development* **128**, 4057–4067.

[175] Friml J, Yang X, Michniewicz M, Weijers D, Quint A, Tietz O, Benjamins R, Ouwerkerk PBF, Ljung K, Sandberg G, Hooykaas PJJ, Palme K *et al.* (2004) A PINOID-dependent binary switch in apical-basal PIN polar targeting directs auxin efflux. *Science* **306**, 862–865.

[176] Blilou I, Xu J, Wildwater M, Willemsen V, Paponov I, Friml J, Heidstra R, Aida M, Palme K & Scheres B (2005) The PIN auxin efflux facilitator network controls growth and patterning in *Arabidopsis* roots. *Nature* **422**, 39–44.

[177] Friml J, Vieten A, Sauer M, Weijers D, Schwarz H, Hamann T, Offringa R & Jürgens G (2003) Efflux-dependent auxin gradients establish the apical-basal axis of *Arabidopsis*. *Nature* **426**, 147–153.

[178] Paponov IA, Teale WD, Trebar M, Blilou I & Palme K (2001) The PIN auxin efflux facilitators: Evolutionary and functional perspectives. *Trends Plant Sci* **11**, 170–177.

[179] Aida M, Beis D, Heidstra R, Willemsen V, Blilou I, Galinha C, Nussaume L, Noh YS, Amasino R & Scheres B (2004) The *PLETHORA* genes mediate patterning of the *Arabidopsis* root stem cell niche. *Cell* **119**, 109–120.

[180] Friml J, Wiśniewska J, Benková E, Mendgen K & Palme K (2002) Lateral relocation of auxin efflux regulator PIN3 mediates tropism in *Arabidopsis*. *Nature* **415**, 806–809.

[181] Xu J & Scheres B (2005) Dissection of Arabidopsis ADP-RIBOSYLATION FACTOR 1 function in epidermal cell polarity. *Plant Cell* **17**, 525–536.

[182] Wenzel CL, Schuetz M, Yu Q & Mattsson J (2007) Dynamics of *MONOPTEROS* and PIN-FORMED1 expression during leaf vein pattern formation in *Arabidopsis thaliana*. *Plant J* **49**, 387–398.

[183] Roussel CJ & Roussel MR (2003) Generic object-oriented differential equation integrators. *C/C++ Users J* **21** (11), 18–23.

[184] Kramer EM (2004) PIN and AUX/LAX proteins: Their role in auxin accumulation. *Trends Plant Sci* **9**, 578–582.

[185] Liscum E & Reed JW (2002) Genetics of Aux/IAA and ARF action in plant growth and development. *Plant Mol Biol* **49**, 387–400.

[186] Overvoorde PJ, Okushima Y, Alonso JM, Chan A, Chang C, Ecker JR, Hughes B, Liu A, Onodera C, Quach H, Smith A, Yu G *et al.* (2005) Functional genomic analysis of the *AUXIN/INDOLE-3-ACETIC ACID* gene family members in *Arabidopsis thaliana*. *Plant Cell* **17**, 3282–3300.

[187] Parry G & Estelle M (2006) Auxin receptors: A new role for F-box proteins. *Curr Op Cell Biol* **18**, 152–156.

[188] Schrader J, Baba K, May S, Palme K, Bennett M, Bhalerao RP & Sandberg G (2003) Polar auxin transport in the wood-forming tissues of hybrid aspen is under simultaneous control of developmental and environmental signals. *Proc Natl Acad Sci USA* **100**, 10096–10101.

[189] Peer WA, Bandyopadhyay A, Blakeslee JJ, Makam SN, Chen RJ, Masson PH & Murphy AS (2004) Variation in expression and protein localization of the PIN family of auxin efflux facilitator proteins in flavonoid mutants with altered auxin transport in *Arabidopsis thaliana*. *Plant Cell* **16**, 1898–1911.

[190] Sieberer T, Seifert GJ, Hauser MT, Grisafi P, Fink GR & Luschnig C (2000) Post-transcriptional control of the *Arabidopsis* auxin efflux carrier EIR1 requires AXR1. *Curr Biol* **10**, 1595–1598.

[191] Abas L, Benjamins R, Malenica N, Paciorek T, Wiśniewska J, Moulinier-Anzola JC, Sieberer T, Friml J & Luschnig C (2006) Intracellular trafficking and proteolysis of the *Arabidopsis* auxin-efflux facilitator PIN2 are involved in root gravitropism. *Nat Cell Bio* **8**, 249–256.

[192] Uggla C, Moritz T, Sandberg G & Sundberg B (1996) Auxin as a positional signal in pattern formation in plants. *Proc Natl Acad Sci USA* **93**, 9282–9286.

[193] Groover AT, Pattishall A & Jones AM (2003) *IAA8* expression during vascular cell differentiation. *Plant Mol Biol* **51**, 427–435.

[194] Campbell NA & Reece JB (2002) *Biology*. Sixth edn. Benjamin Cummings, Toronto.

[195] Campanoni P, Blasius B & Nick P (2003) Auxin transport synchronizes the pattern of cell division in a tobacco cell line. *Plant Physiol* **133**, 1251–1260.

[196] Friml J, Benková E, Blilou I, Wisniewska J, Hamann T, Ljung K, Woody S, Sandberg G, Scheres B, Jürgens G & Palme K (2002) AtPIN4 mediates sink-driven auxin gradients and root patterning in *Arabidopsis*. *Cell* **108**, 661–673.

[197] Friml J (2003) Auxin transport – shaping the plant. *Curr Op Plant Biol* **6**, 7–12.

[198] Berleth T & Sachs T (2001) Plant morphogenesis: Long-distance coordination and local patterning. *Curr Op Plant Biol* **4**, 57–62.

[199] Izhaki A & Bowman JL (2007) KANADI and Class III HD-Zip gene families regulate embryo patterning and modulate auxin flow during embryogenesis in *Arabidopsis*. *Plant Cell* **19**, 495–508.

[200] Schwöppe C, Winkler HH & Neuhaus HE (2003) Connection of transport and sensing by UhpC, the sensor for external glucose-6-phosphate in *Escherichia coli*. *Eur J Biochem* **270**, 1450–1457.

[201] Luschnig C (2001) Auxin transport: Why plants like to think BIG. *Curr Biol* **11**, R831–R833.

[202] Ljung K, Hull AK, Kowalczyk M, Marchant A, Celenza J, Cohen JD & Sandberg G (2002) Biosynthesis, conjugation, catabolism and homeostasis of indole-3-acetic acid in *Arabidopsis thaliana*. *Plant Mol Biol* **49**, 249–272.

[203] Aloni R, Schwalm K, Langhans M & Ullrich CI (2003) Gradual shifts in sites of free-auxin production during leaf-primordium development and their role in vascular differentiation and leaf morphogenesis in *Arabidopsis*. *Planta* **216**, 841–853.

[204] Secko D (2007) Auxin receptor hides in plain sight. *The Scientist* **21**, 69.

[205] Somerville C & Meyerowitz E, eds. (2002) *The Arabidopsis Book*. American Society of Plant Biologists, Rockville, MD. http://www.aspb.org/publications/arabidopsis/.

[206] Meyerowitz EM & Somerville CR, eds. (1994) *Arabidopsis*. Cold Spring Harbor Laboratory Press, Plainview, NY.

[207] Davies PJ, ed. (1995) *Plant Hormones: Physiology, Biochemistry and Molecular Biology*. 2nd edn. Kluwer Academic Publishers, Boston.

[208] Davies PJ, ed. (2004) *Plant Hormones: Biosynthesis, Signal Transduction, Action!* Kluwer Academic Publishers, Boston.